

A Thesis on
Numerical Study of Crystallization Process Using CFD Tools

Submitted by

Prasanna Rao Ravi

Roll No. 211CH1263

In partial fulfillment of the requirements for the degree in
Master of Technology in Chemical Engineering

Under the Supervision of

Dr. BasudebMunshi



Department of Chemical Engineering
National Institute of Technology, Rourkela

May, 2013



DEPARTMENT OF CHEMICAL ENGINEERING
NATIONAL INSTITUTE OF TECHNOLOGY, ROURKELA
ODISHA, INDIA – 769008

CERTIFICATE

This is to certify that the thesis titled “**Numerical Study of Crystallization Process using CFD Tools**”, submitted to the National Institute of Technology, Rourkela by **Prasanna Rao Ravi**, Roll No. **211CH1263** for the award of the degree of **Master of Technology** in Chemical Engineering, is a bonafide record of research work carried out by him under my supervision and guidance. The candidate has fulfilled all the prescribed requirements. The thesis, which is based on candidate’s own work, has not been submitted elsewhere for a degree/diploma.

Date: 24/05/2013

Dr. Basudeb Munshi

Associate Professor

Department of Chemical Engineering
National Institute of Technology, Rourkela

ACKNOWLEDGEMENTS

I would like to express my sincere gratitude to Dr. Basudeb Munshi for his guidance and assistance in this thesis. The technical discussions with Dr. Basudeb Munshi were always been very insightful, and I will always be indebted to his for all the knowledge he shared with me. His prompt responses and availability despite his constantly busy schedule were truly appreciated. The reality is that Dr. Basudeb Munshi was much more than an advisor for me. His encouragement and efforts led this report to successful completion in a timely fashion.

Special Thanks also to Mr. Akhilesh Khapre for sharing the literature and invaluable assistance.

I am also thankful to all the staff and faculty members of Chemical Engineering Department, National Institute of Technology, Rourkela for their consistent encouragement.

I would like to extend my sincere thanks to my friends and colleagues.

Date: 24/05/2013

Prasanna Rao Ravi
Roll No. 211CH1263
4th Semester, M.Tech
Chemical Engineering Dept

INDEX

ABSTRACT	i
LIST OF FIGURES	ii
LIST OF TABLES	v
NOMENCALTURE	vi
CHAPTERS	
<hr/>	
1. INTRODUCTION	
1.1 Methods to generate supersaturation	2
1.2 Solubility curve	3
1.3 Nucleation	4
1.4 Computational Fluid Dynamics	4
1.4.1 Ansys Fluent software	5
1.4.2 Advantages of CFD	6
1.4.3 Limitations of CFD	6
1.5 Objectives	7
1.6 Organization of the thesis	7
2. LITERATURE SURVEY	
2.1 Literature review on crystallization	9
2.2 Literature review on numerical solution of population balance equation	13

3. COMPUTATIONAL FLUID DYNAMICS MODEL EQUATIONS	
3.1 Eulerian Model	15
3.2 Population balance model	18
4. Crystallization of sucrose	
4.1 Problem statement	20
4.2 Geometry and mesh	21
4.3 Initial and Boundary conditions, and Solution schemes	22
4.4 Results and discussion	23
5. Conclusion and future scope	40
6. References	41

ABSTRACT

Crystallization is the formation of solid particles within a homogenous phase. Crystallization is considered a last stage purification step in pharmaceutical, chemical, agrochemical and food industries. Crystallization is mostly used for separation of a pure product from an impure solution and the product formed is suitable for packing and marketing. Good yield and purity are important for crystallization; apart from it crystal size distribution also plays a vital role in the design of crystallization. The energy required for crystallization is less than distillation. The study is made on crystallization process of sucrose in a continuous rectangular flow chamber. The present work is aimed to compare the simulation results with experimental results and to study the parametric sensitivity on mean crystal diameter of sucrose and total crystal production with variation in inlet velocity of solution, inlet mass fraction of sucrose and wall temperature of crystallizer. The transient simulations are carried out to study the crystallization process. The simulation results when validated against experimental results are found to be consistent. The simulation results show that as the inlet mass fraction of sucrose is increased, then the mean crystal size and total crystal production are observed to be increased. The mean crystal size is increased and total crystal production is decreased with decrease in inlet velocity of solution. The mean crystal size is observed to be invariant with change in wall temperature of the crystallizer but the total crystal production is increased with increase in wall temperature.

Keywords: CFD, Crystallization, Mean crystal Size, Total crystal production

LIST OF FIGURES

Figure No.	Figure Caption	Page No.
Figure 1.1	Ostwald –Miers diagram for solute/solvent	3
Figure 2.1	The crystallization triangle (Jones, 2002)	12
Figure 4.1	Schematic diagram of nucleation cell	20
Figure 4.2	Geometry of the crystallizer in ANSYS workbench	22
Figure 4.3	Tetrahedral mesh of the crystallizer geometry	22
Figure 4.4	Transient distributions of local crystal diameter at location 0.015m from inlet and mean crystal diameter. The used inlet velocity is 0.001067 m/s, inlet mass fraction of sucrose is 0.7 and inlet temperature is 303.15K.	24
Figure 4.5	Distribution of moment-0 inside the crystallizer at time 240.9 second. The used inlet velocity is 0.001067 m/s, inlet mass fraction of sucrose is 0.7 and inlet temperature is 303.15K. The outlet is present at 0.0 m.	24
Figure 4.6	Distribution of moment-3 inside the crystallizer at 400 second. The used inlet velocity is 0.001067 m/s, inlet mass fraction of sucrose is 0.7 and inlet temperature is 303.15K. The outlet is present at 0.0 m.	25
Figure 4.7	Distribution of velocity inside the crystallizer at 400 second. The used inlet velocity is 0.001067 m/s, inlet mass fraction of sucrose is 0.7 and inlet temperature is 303.15K. The outlet is present at 0.0 m.	25
Figure 4.8	Effect of inlet mass fraction of sucrose on the transient distribution of mean crystal diameter. The used inlet velocity is 0.001067 m/s and the inlet temperature is 303.15K.	26

Figure 4.9	Contour plot of moment-3 of the crystallizer at time 360second. The used inlet velocity is 0.001067 m/s, inlet mass fraction of sucrose is 0.78 and the inlet temperature is 303K. The outlet is present at 0.0 m.	27
Figure 4.10	Transient distribution of mean crystal diameter obtained by TVAC/TSAC and TLAC/TNAC. The used inlet mass fraction of sucrose is 0.85,the inlet temperature is 303.15K and the inlet velocity is 0.001067 m/s.	27
Figure 4.11	Transient distribution of mean crystal diameter obtained by TVAC/TSAC and TLAC/TNAC. The used inlet mass fraction of sucrose is 0.78,the inlet temperature is 303.15K and the inlet velocity is 0.001067 m/s.	28
Figure 4.12	Transient distribution of mean crystal diameter obtained by TVAC/TSAC and TLAC/TNAC. The used inlet mass fraction of sucrose is 0.74,the inlet temperature is 303.15K and the inlet velocity is 0.001067 m/s.	29
Figure 4.13	Transient distribution of mean crystal diameter obtained by TVAC/TSAC and TLAC/TNAC. The used inlet mass fraction of sucrose is 0.70,the inlet temperature is 303.15K and the inlet velocity is 0.001067 m/s.	30
Figure 4.14	Effect of inlet mass fraction of sucrose on the transient distribution of number density of the crystallizer. The used inlet velocity of solution is 0.001067 m/s and the inlet temperature is 303.15K.	31
Figure 4.15	Effect of the inlet velocity on the transient distribution of mean crystal diameter inside the crystallizer. The used inlet mass fraction of sucrose is 0.7 and the inlet temperature is 303.15K.	32
Figure 4.16	Transient distribution of mean crystal diameter obtained by TVAC/TSAC and TLAC/TNAC. The used inlet mass fraction of sucrose is 0.7,the inlet temperature is 303.15K and the inlet velocity is 0.0005 m/s.	32
Figure 4.17	Transient distribution of mean crystal diameter obtained by TVAC/TSAC and TLAC/TNAC. The used inlet mass fraction of sucrose is 0.7,the inlet temperature is 303.15K and the inlet velocity is 0.0001 m/s.	33

Figure 4.18	Transient distribution of mean crystal diameter obtained by TVAC/TSAC and TLAC/TNAC. The used inlet mass fraction of sucrose is 0.7, the inlet temperature is 303.15K and the inlet velocity is 0.00001 m/s.	34
Figure 4.19	Transient distribution of mean crystal diameter obtained by TVAC/TSAC and TLAC/TNAC. The used inlet mass fraction of sucrose is 0.7, the inlet temperature is 303.15K and the inlet velocity is 0.001 m/s.	35
Figure 4.20	Effect of inlet velocity on the transient distribution of number density of crystals. The used inlet mass fraction of sucrose is 0.7 and the inlet temperature is 303.15K.	35
Figure 4.21	Effect of the wall temperature of the crystallizer on the transient distribution of number density of the crystals inside the crystallizer. The used inlet mass fraction of sucrose is 0.7, the inlet temperature is 303.15 K and the inlet velocity is 0.001m/s.	36
Figure 4.22	Effect of the wall temperature of the crystallizer on the transient distribution of mean crystal diameter. The used inlet mass fraction of sucrose is 0.7, the inlet temperature is 303.15 K and the inlet velocity is 0.001m/s.	37
Figure 4.23	Transient distribution of mean crystal diameter obtained by TVAC/TSAC and TLAC/TNAC. The used inlet mass fraction of sucrose is 0.7, the inlet temperature is 303.15K and the inlet velocity is 0.001067 m/s. The specified wall temperature is 323 K.	38
Figure 4.24	Transient distribution of mean crystal diameter obtained by TVAC/TSAC and TLAC/TNAC. The used inlet mass fraction of sucrose is 0.7, the inlet temperature is 303.15K and the inlet velocity is 0.001067 m/s. The specified wall temperature is 333 K.	38
Figure 4.25	Contour plot of the temperature of the crystallizer at time 360second. The used inlet velocity of is 0.001067 m/s, inlet mass fraction of sucrose is 0.70 and the inlet temperature is 303.15K. The specified wall temperature is 333 K. The outlet is present at 0.0 m.	39
Figure 4.26	Contour plot of moment-3 of the crystallizer at time 360second. The used inlet velocity is 0.001067 m/s, inlet mass fraction of sucrose is 0.70 and the inlet temperature is 303.15K. The specified wall temperature is 333 K. The outlet is present at 0.0 m.	39

LIST OF TABLES

Table No.	Table Caption	Page No.
1) Table 4.1:	Physical dimensions and operating conditions used in simulation.	21
2) Table 4.2:	Discretization schemes for modeling equations	23

NOMENCLATURE

Y_i	mass fraction
∇	gradient
C	concentration
D	diffusion coefficient
E	activation energy
p	static pressure
R	rate of the reaction
Sc	Schmidt number
t	time
T	temperature
TLAC	total length of all crystals per unit volume of solution
TNAC	total number of all crystals per unit volume of solution
TSAC	total surface of all crystals per unit volume of solution
TVAC	total volume of all crystals per unit volume of solution
v	velocity
α	volume fraction
μ	viscosity

Subscripts

j	species
p,q	phase
r	reaction
t	turbulent

CHAPTER 1

INTRODUCTION

CHAPTER 1**INTRODUCTION**

Crystallization is the formation of solid particles within a homogenous phase. Solid particles can be formed from either vapor phase or liquid phase through crystallization (Abbas et al., 2007). Crystals formed during crystallization from an impure solution are itself pure and crystals formed are also suitable for packing and storing. More than 80% of the substances used in pharmaceuticals, fine chemicals, agrochemicals, food and cosmetics are isolated or formulated in their solid form.

The driving force for crystallization from solution is supersaturated solution. If the solute concentration exceeds the equilibrium (saturated) solute concentration at a fixed temperature, then the solution is said to be supersaturated solution. Formation of crystal is considered in general a two-step process. Former is formation of nuclei known as nucleation and latter is growth of these nuclei to macroscopic scale known as crystal growth. The formation of crystal is governed by nucleation rate and birth rate. Nucleation rate and birth rate are the crystallization kinetics (Abdel et al., 2003)

1.1 Methods to generate supersaturation

Based on solubility of solute dependence on temperature, four methods have been classified.

1. Temperature reduction,
2. Evaporating the solvent,
3. Changing the solvent composition(salting) and
4. Chemical reaction(precipitation)

If the solubility increases more or less with temperature as in case of KNO_3 , then the supersaturated solution can be generated by simply decrease in temperature. If the solute solubility is relatively invariant with temperature, then the supersaturated solution can formed by evaporating a small portion of the solvent (increasing the temperature). If neither evaporation nor temperature reduction is desirable then a third component is added which physically forms with

the original solvent, a mixed solvent where the solubility of the solvent is sharply reduced. A new insoluble solute can also be formed by reaction the third component with the original solute in the solution. This process is called precipitation (Julian et al., 1993).

1.2 Solubility curve

The Ostwald-Miers diagram illustrates the basis of all methods of solution growth. The solid line represents a section of the curve for the solute / solvent system. The upper dashed line is referred to as the super-solubility line and denotes the temperatures and concentration where spontaneous nucleation occurs (Mullin, 1993).

The diagram can be evaluated on the basis of three zones:

- The stable (unsaturated) zone where crystallization is impossible,
- The metastable (supersaturated) zone where spontaneous nucleation is improbable but a crystal located in this zone will grow and
- The unstable or labile (supersaturated) zone where spontaneous nucleation is probable and so the growth.

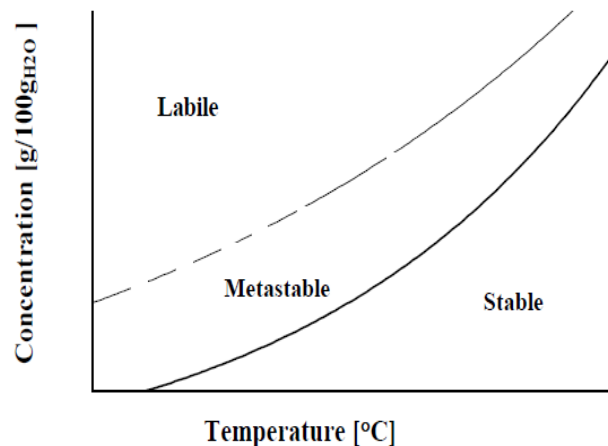


Figure 1.1: Ostwald –Miers diagram for solute/solvent (Mullin, 1993)

1.3 Nucleation

The nucleation rate is the number of new particles formed per unit time per unit volume of magma or solid free mother liquor (Julian et al., 1993). Nucleation is classified into three types.

1. Primary nucleation,
2. Secondary nucleation and
3. Contact nucleation.

Primary nucleation refers to the birth of very small bodies (nuclei) of a new phase within a supersaturated homogenous existing phase. In primary nucleation some energy is consumed to form an interface, based on the surface energy of each phase, so more energy is required for the nucleation and it is advisable to go for secondary nucleation

Secondary nucleation refers to the formation of nuclei attributable to the influence of the existing macroscopic crystals in the magma is called secondary nucleation. In secondary nucleation, crystal growth can also be influenced by fluid shear and collisions between existing crystals with each other or with the walls of the crystallizer and rotary impeller or agitator blades.

In contact nucleation the crystals are forced to strike on the selected crystal surface by small rods in laboratory scale. The energy required for contact nucleation is less when compared to primary and secondary nucleation so no visible effect can be observed.

1.4 Computational Fluid Dynamics

Computational Fluid Dynamics (CFD) is the art of replacing such PDE systems by a set of algebraic equations which can be solved using digital computers. Fluid flow is governed by conservation laws of energy, mass and momentum. These are usually a set of partial differential equations. CFD gives a qualitative and quantitative prediction of fluid flow by numerical solution of partial differential equations. In CFD, the flow domain is divided into small grids or elements. Differential equations of mass, momentum and energy balance are discretized and

represented in terms of the variables at any predetermined position within the or at the center of cell. Finally, the initial conditions and the boundary conditions of the specific problem are used to solve these equations. The solution method can be direct or iterative. In addition, certain control parameters are used to control the convergence, stability, and accuracy of the method. These equations are solved iteratively until the solution reaches the desired accuracy (ANSYS Fluent 13.0).

1.4.1 Ansys Fluent software

Fluent is one of the widely used CFD software package. Ansys Fluent software contains the wide range of physical modeling capabilities which are needed to model flow, turbulence, reactions and heat transfer for industrial applications.

Features of Ansys Fluent software:

- **Turbulence:** Ansys Fluent offers a number of turbulence models to study the effects of turbulence in a wide range of flow regimes.
- **Multiphase flow:** It is possible to model different fluids in a single domain with FLUENT.
- **Acoustics:** It allows users to perform sound calculations.
- **Reacting flow:** Modeling of surface chemistry, combustion as well as finite rate chemistry can be done in fluent.
- **Mesh flexibility:** Ansys Fluent software provides mesh flexibility. It has the ability to solve flow problems using unstructured meshes. Mesh types that are supported in FLUENT includes triangular, quadrilateral, tetrahedral, hexahedral, pyramid, prism (wedge) and polyhedral. The techniques which are used to create polyhedral meshes save time due to its automatic nature. A polyhedral mesh contains fewer cells than the corresponding tetrahedral mesh. Hence convergence is faster in case of polyhedral mesh.

- Dynamic and moving mesh: The user sets up the initial mesh and instructs the motion, while FLUENT software automatically changes the mesh to follow the motion while FLUENT software automatically changes the mesh to follow the motion instructed.
- Post-processing and data export: Users can post-process their data in Fluent software, creating among other things contours, path lines, and vectors to display the data.

1.4.2 Advantages of CFD

- Computational simulations are relatively inexpensive, and costs are likely to decrease as computers become more powerful.
- CFD simulations can be executed in a short period of time.
- CFD allows the analyst to examine a large number of locations in the region of interest, and yields a comprehensive set of flow parameters for examination.
- CFD allows great control over the physical process, and provides the ability to isolate specific phenomena for study. (Example: a heat transfer process can be idealized with adiabatic, constant heat flux, or constant temperature boundaries)

1.4.3 Limitations of CFD

- CFD solutions rely upon physical models of real world processes (e.g. turbulence, chemistry, multiphase flow, compressibility, etc.).
- Solving equations on a computer invariably introduces numerical errors.
- As with physical models, the accuracy of the CFD solution is only as good as the initial/boundary conditions provided to the numerical model.

1.5 Objectives

The research objective can be broadly divided into following sub-sections:

- i. Modeling and simulation of sucrose crystallization process
- ii. Validation of the model by comparing the present simulated results with the data available in the open literature.
- iii. Studying the effect of inlet velocity of the solution, inlet mass fraction of sucrose and wall temperature of the crystallizer on the size and total production of the crystals in the crystallizer.

1.6 Organization of the thesis

Chapter 1 represents the basics of crystallization including the methods to generate supersaturation, types of nucleation and application and role of computational fluid dynamics.

Chapter 2 deals with the literature review of crystallization. The chapter is divided into the sections namely literature review on crystallization and literature review on numerical solution of population balance equation.

Chapter 3 comprises of modeling equations of multiple phase flow and population balance. The model equation includes the equation of continuity, momentum and energy.

Chapter 4 represents the study of crystallization of sucrose using CFD tools. The modeling equations are solved numerically to study the effects of inlet velocity of solution, inlet mass fraction of sucrose and wall temperature of crystallizer on mean crystal diameter and total crystal production.

Chapter 5 deals with the overall conclusions and future recommendations.

CHAPTER2

LITERATURE SURVEY

CHAPTER 2**LITERATURE SURVEY**

A substantial quantity of research work is done on crystallization both experimentally and numerically. But some research works are completely experimental and others include mostly theoretical works. There is little research activity which took care both the types. It forces us to look into the grey area of crystallization process. This chapter deals with the literature review of crystallization and its related processes. It is divided into two sections:

1. Literature review on crystallization
2. Literature review on numerical solution of population balance equation

2.1 Literature review on crystallization

Crystallization is the formation of solid particles from a homogenous solution and in general it is a solid- liquid separation technique (Angelov et al., 2007; Basim et al., 2002). It is widely used in pharmaceutical, chemical, agrochemical and food industries (Lindberg et al., 2001; Hussain et al., 2004). The driving force for crystallization is supersaturation. A solution is said to be supersaturated if the concentration of solute is more than the saturated concentration of it at the prevailing temperature. Neither birth of nuclei nor crystal growth will occur when the solution is in unsaturated condition (Julain et al., 1993).

The supersaturated solution can be generated by changing some system properties like P^H , temperature, solution composition or by adding a third component (Andre et al., 2011). The selection of the system property depends upon the variation of solubility of solute with temperature in the solvent. If the solubility increases more or less with temperature as in case of KNO_3 and Na_2SO_4 (Deckelmann et al, 2007) then the supersaturated solution can be generated by simply decreasing the system temperature. If the solute solubility is relatively invariant with temperature, then the supersaturated solution can be formed by evaporating a small portion of the solvent (increasing the temperature) as in case of $NaCl$. If neither evaporation nor temperature reduction was desirable then a third component is added which physically forms with the original

solvent, a mixed solvent where the solubility of the solvent is sharply reduced, otherwise the third component was added such that a new insoluble solute can be formed by reaction of the third component with the original solute in the solution. This process is called precipitation (Julian et al., 1993).

The transfer of the molecules from the continuous phase (solution) to the solid phase is governed by nucleation and growth rates. Both the rates are called the crystallization kinetics (Basim et al., 2002; Bernado et al., 2011).

Nucleation which was defined as birth of new particles per unit volume of magma or solid free mother liquor (Julian et al., 1993) can be distinguished into two types namely primary and secondary nucleation. Primary nucleation refers to the birth of very small bodies of a new phase within a supersaturated homogenous solution and if the birth was uninfluenced by foreign particles or wall of the crystallizer, then the primary nucleation was termed as homogenous nucleation otherwise the primary nucleation was termed as heterogeneous nucleation (Albert et al., 1993). In primary nucleation some energy was consumed to form an interface, based on the surface energy of each phase, so more energy was required for the primary nucleation and it was advisable to go for secondary nucleation where nucleation was induced mainly by existing macroscopic crystals (seeds) and also by fluid flow, crystal disruption etc. (Jones, 2002) and secondary nucleation can be carried out at low supersaturations. Grinding processes are employed to generate seed crystals but the mean size and size distribution of seeds are unsatisfactory. Also the grinding process may impart some impurities during grinding and even pollute the environment. These undesirable characteristics do not appear in the seeds that are formed by insonated nucleation (Kordylla et al, 2008; Corona et al., 2010). Insonated nucleation was the effect of ultra sound to control the nucleation rate. The ultrasonic effect on crystallization has been reported to accelerate crystal precipitation, retard precipitation, change the crystal size distribution and crystal habit, increase nucleation rate and agglomerate particles (Hairong et al., 2006; Guo et al., 2006; Jones et al., 2011).

The mechanism of crystal growth from solution is often thought to consist of two steps in series, i.e., a mass transfer diffusion step followed by a surface reaction step (Shiau, 2003; Tai, 1999). The crystal growth rate can be expressed as rate of linear increase in characteristic length or mass deposition rate, mass flux (Jones, 2002). The mechanism of crystal growth has been

proposed by several theoretical models. The theoretical models can be broadly classified into two types namely diffusion-reaction model and surface integration model.

The diffusion-reaction model (Julian et al., 1993; Jones, 2002) evaluates individual mass transfer coefficient, surface reaction coefficient and order of the growth rate. The growth rate can be expressed as

$$\frac{dM_c}{dt} = k_g A (C - C^*)^g \quad (2.1)$$

Where $\frac{1}{k_g} = \frac{1}{k_r} + \frac{1}{k_d}$, M_c is crystal mass, t is time, k_g is overall coefficient, g is growth rate order, A is interfacial area, k_d is diffusion coefficient, k_r is surface rate constant, C is supersaturated concentration of solute and C^* is saturated concentration of solute. Based on this model growth rate equation was derived for potash alum but only stated the growth rate order i.e., 2 (Tai, 1999) and the growth rate order for potassium sulphate (Das et al., 1974) is 2.4. But between the theoretical and experimental growth rate a large difference was found. So models based surface integration has been proposed and among the surface integration model the screw dislocation or BCF (Burton-Cabrera-Frank) model has been frequently used. The BCF model proposed that the sliding of crystals on the crystal surface creates a ramp or stair case structure on the crystal surface called dislocalities which affect the crystal growth (Bento et al., 2010). The structure was like a two dimensional and the corners act like a kink where the crystal strives to fits itself. The BCF model given the expression for growth rate (G) as

$$G = Y \left(\frac{\sigma_i^r}{\delta} \right) \tanh \left(\frac{\delta}{\sigma_i} \right) \quad (2.2)$$

Where Y and δ are complex temperature-dependent constants, σ_i was the relative supersaturation at the solution/crystal interface.

Growth rate based on surface integration step for all ranges of supersaturation is often correlated using a power law as

$$G = k_r \sigma_i^r \quad (2.3)$$

Where k_r was surface rate constant.

On further simplification done by Shiau, 2003 the mean growth rate can be written as

$$\bar{G} = \bar{a}k_0 \exp\left(\frac{-E}{RT}\right)\sigma^r \quad (2.4)$$

Where \bar{a} was average dislocation activity (dimensionless), k_0 was average frequency factor ($\mu\text{m}/\text{min}$), E was activation energy (kJ/mol), R was universal gas constant(kJ/mol.K), σ was relative supersaturation and T was temperature(K)

For sucrose the meangrowth rate equation(Shiau, 2003) was stated as

$$\bar{G} (\mu\text{m}/\text{min}) = 2.68 * 10^{12} \exp\left(\frac{-66.6}{RT}\right)\sigma^{1.32} \quad (2.5)$$

Apart from crystallization kinetics, the crystal size distribution plays a vital role in the design of crystallizer and if further processing of the crystals is desired, large crystals with uniform size are important for washing, filtering, transportation, and storage. Jones, 2002described that the kinetics (birth rate, growth rate) and residence time (volume of crystallizer, volumetric flow rate) are the important parameters in estimating the crystal size distribution.

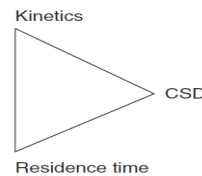


Figure 2.1: The crystallization triangle (Jones, 2002)

Type of crystallizer to choose depends on chemical nature of crystal product, crystal product quality, range of crystallizer size distribution, shape of crystal product etc. Darmont et al., 1992 invented a batch crystallizerfor an inorganic substance like NaClwhich can be used for production of a approximately spherical shape crystal and non agglomerating crystal is required, Sexar, 1984 invented a fractional crystallizer which can be used for production of a very large numbers of crystal products at low investment cost and at low energy consumption and Verdoes et al., 2007 invented a continuous crystallizer for the production of constant product quality in very narrow size particle size distribution and in smaller reactor volume.

2.2 Literature review on numerical solution of population balance equation

Alone mass balance, momentum and energy balance does not give any information regarding crystal size distribution. The conservation laws are unchanged even if product was one large crystal or some number of small crystals (Julian et al., 1993)

The crystal size distribution can evolve in conjunction with transport and chemical reaction in a multiphase system. The evolutionary processes can be a combination of different phenomena like nucleation, growth, dispersion, dissolution, aggregation, and breakage producing the dispersion. Thus in multiphase flow involving a size distribution, a balance equation is required to describe the changes in the particle population, in addition to momentum, mass, and energy balances. This balance was generally referred to as the population balance. Average particle size can be evaluated from the population balance equation (PBE).

Numerical solution of PBE was done by adaptive high-resolution finite volume schemes (Angelov et al., 2007; Angelov et al., 2009; Angelov et al., 2006), method of characteristics (Angelov et al., 2009; Gerald et al., 2007; Ramkrishna et al., 1997), classes method (Daniele et al., 2005), quadratic method of moment (Daniele et al., 2005) and semidiscrete upwind scheme (Gerald et al., 2007).

Numerical solution of PBE by high-resolution finite volume scheme, shown accuracy and efficiency in resolving sharp peak and accuracy increased further with the adaptive meshing techniques when compared with finite volume schemes. Unlike first-order schemes, these high resolution schemes give less numerical diffusion and also avoid the numerical dispersion which can happen in the high order schemes near sharp discontinuities. The numerical test cases presented by Angelov et al., 2006 shows that these high resolution schemes also worked well for the solution of PBEs with nucleation and size dependent/independent growth. The numerical solution of PBE by method of characteristics (Angelov et al., 2006; Ramkrishna et al., 1997) also has overcome the numerical diffusion and dispersion and also gave highly resolved solutions, as well as being computationally efficient. Classes method (CM) also gave good accuracy like high-resolution finite volume scheme and method of characteristics but the number of scalars are more and more computational time is required (Daniele et al., 2005). Semi-discrete finite volume

scheme (FVS) scheme for the numerical solution of PBE also showed the same results like method of characteristics and high resolution finite volume scheme(Gerald et al., 2009).

A study was made by using CFD tool in a jet crystallizer by Reginald et al.,2009. The simulation results of the shape of the crystal size distribution and its variation with Re number is found consistent with experimental results. The simulation results indicate that more and larger crystals, with wider size distribution, were produced at a lower jet Reynolds number due to a longer residence time for nucleation and growth.

CHAPTER 3

COMPUTATIONAL FLUID DYNAMICS MODEL EQUATIONS

COMPUTATIONAL FLUID DYNAMICS MODEL EQUATIONS

In this chapter the computational fluid dynamics modeling equations are described for multiphase system. Besides, population balance modeling equations are also mentioned. The theory for the system is taken from the ANSYS Fluent 13.0.

3.1 Eulerian Model

A large number of flows encountered in nature and technology are a mixture of phases. Physical phases of matter are gas, liquid, and solid, but the concept of phase in a multiphase flow system is applied in a broader sense. In multiphase flow, a phase can be defined as an identifiable class of material that has a particular inertial response to and interaction with the flow and the potential field in which it is immersed.

Mass conservation equation

The continuity equation for phase q is

$$\frac{\partial}{\partial t} (\alpha_q \rho_q) + \nabla \cdot (\alpha_q \rho_q \vec{v}) = \sum_{p=1}^n (\dot{m}_{pq} - \dot{m}_{qp}) + S_q \quad (3.1)$$

Where α_q the volume fraction of qth phase, \vec{v} is the velocity of phase q, \dot{m}_{pq} characterizes the mass transfer from the pth to qth phase and \dot{m}_{qp} characterizes the mass transfer from the qth to pth phase

Species transport equations

The species transport equation of phase i is

$$\frac{\partial}{\partial t} (\rho Y_i) + \nabla \cdot (\rho \vec{v} Y_i) = \nabla \cdot \vec{J}_i + R_i + S_i \quad (3.2)$$

R_i is the net rate of production of species i by chemical reaction, Y_i is mass fraction of species i and S_i is the rate of creation by addition from the dispersed phase plus any user-defined sources. An equation of this form will be solved for N-1 species where N is the total number of fluid

phase chemical species present in the system. Since the mass fraction of the species must sum to unity, the N^{th} mass fraction is determined as one minus the sum of the $N-1$ solved mass fractions.

Mass diffusion in laminar flows:

J_i is the diffusion flux of species i , which arises due to concentration gradients.

$$\vec{J}_i = -\rho \cdot D_{m,i} \nabla Y_i \quad (3.3)$$

Mass diffusion in turbulent flows

$$\vec{J}_i = -\left(\rho \cdot D_{m,i} + \frac{\mu_t}{Sc}\right) \nabla Y_i \quad (3.4)$$

Momentum conservation equation

The momentum balance for phase q is

$$\begin{aligned} \frac{\partial}{\partial t} (\alpha_q \rho_q \vec{v}_q) + \nabla \cdot (\alpha_q \rho_q \vec{v}_q \vec{v}_q) = & -\alpha_q \nabla p + \nabla \cdot \bar{\tau}_q + \alpha_q \rho_q \vec{g} + \sum_{p=1}^n (\vec{R}_{pq} + \dot{m}_{pq} \vec{v}_{pq} - \dot{m}_{qp} \vec{v}_{qp}) + \\ & (\vec{F}_q + \vec{F}_{lift,q} + \vec{F}_{vm,q}) \end{aligned} \quad (3.5)$$

Where $\bar{\tau}_q$ is the q^{th} phase stress-strain tensor, \vec{F}_q is an external body force, $\vec{F}_{lift,q}$ is a lift force, $\vec{F}_{vm,q}$ is a virtual mass force, \vec{R}_{pq} is an interaction force between phases, \vec{v}_{pq} is the interphase velocity, and p is the pressure shared by all phases.

$$\bar{\tau}_q = \mu_q \alpha_q \left[\left(\nabla \vec{v}_q + \nabla \vec{v}_q^T \right) + \alpha_q \left(\lambda_q - \frac{2}{3} \mu_q \right) \nabla \cdot \vec{v}_q \right] \quad (3.6)$$

where μ_q and λ_q are the shear and bulk viscosity of phase q .

Conservation of energy equation

The energy balance for phase q is

$$\begin{aligned} \frac{\partial}{\partial t} (\alpha_q \rho_q h_q) + \nabla \cdot (\alpha_q \rho_q \vec{v}_q h_q) = & -\alpha_q \frac{\partial}{\partial t} (p_q) + \bar{\tau}_q \cdot \nabla \vec{v}_q - \nabla \vec{q}_q + S_q + \sum_{p=1}^n (\vec{Q}_{pq} + \dot{m}_{pq} \vec{v}_{pq} - \\ & \dot{m}_{qp} \vec{v}_{qp}) \end{aligned} \quad (3.7)$$

Where h_q is the specific enthalpy of the qth phase, \vec{q}_q is the heat flux, S_q is a source term that includes sources of enthalpy, \vec{Q}_{pq} is the intensity of heat exchange between the pth and qth phases.

Volume fraction equation

The tracking of the interface(s) between the phases is accomplished by the solution of a continuity equation for the volume fraction of one (or more) of the phases. For the qth (fluid's volume fraction) phase, this equation has the following form

$$\frac{1}{\rho_q} \left[\frac{\partial}{\partial t} (\alpha_q \rho_q) + \nabla \cdot (\alpha_q \rho_q \vec{u}_q) \right] = S_{\alpha q} \sum_{p=1}^n (\dot{m}_{pq} - \dot{m}_{qp}) \quad (3.8)$$

Where \dot{m}_{qp} is the mass transfer from phase q to phase p and \dot{m}_{pq} is the mass transfer from phase p to phase q, α_q is the volume fraction of phase q, ρ_q is density of phase q and \vec{u}_q is the velocity of phase q. By default, the source term on the right-hand side $S_{\alpha q}$ is zero, but we can specify a constant or user-defined mass source for each phase. The volume fraction equation will not be solved for the primary phase; the primary-phase volume fraction will be computed based on the following constraint:

$$\sum_{p=1}^n \alpha_p = 1 \quad (3.9)$$

Material properties

The properties appearing in the transport equations are determined by the presence of the component phases in each control volume. In a two-phase system, for example, if the phases are represented by the subscripts 1 and 2, and the mixture density in each cell is given by

$$\rho = \alpha_2 \rho_2 + (1 - \alpha_2) \rho_1 \quad (3.10)$$

In general, for n phase system, the volume-fraction-averaged density takes on the following form:

$$\rho = \sum \alpha_q \rho_q \quad (3.11)$$

All other properties (e.g., viscosity) are also computed in this manner.

3.2 Population balance model

The population balance model can be applied to crystallization, precipitation reaction from a gas or liquid phase, bubble columns, gas sparging, sprays, fluidized bed polymerization, granulation, liquid-liquid emulsion and separation, and aerosol flows. The population balance equation of secondary phase i is

$$\frac{\partial[\rho_s \alpha_i]}{\partial t} + \Delta \cdot [\rho_s \alpha_i u_i] + \frac{\partial}{\partial V} [G_v \rho_s \alpha_i] = \rho_s V_i (B_{ag,i} - D_{ag,i} + B_{br,i} - D_{br,i}) + 0^i \rho_s V_o \dot{n}_o \quad (3.12)$$

ρ_s is the density of secondary phase and α_i is the volume fraction of secondary phase of particle size i , $B_{ag,i}$ is birth due to aggregation of particle size i , $D_{ag,i}$ is death due to aggregation of particle size i , $B_{br,i}$ is birth due to breakage of particle size i and $D_{br,i}$ is death due to breakage of particle size i , G_v is growth rate and \dot{n}_o is the nucleation rate of particles/ $m^3 \cdot s$.

Moment of secondary phase is given by

$$\text{moment} - i = \sum N_j L_j^i \quad (3.13)$$

($i = 0, 1, 2$ and 3 for moment-0, moment-1, moment-2 and moment-3), N_j is number density of crystal size j and L_j is length of crystal size j .

The volume of a single particle (V) is defined as $K_v L^3$ and the surface area of a single particle, (A) is defined as $K_a L^2$. Where K_v volume is shape factor and K_a is area shape factor.

$$\text{Growth rate } (\mu\text{m}/\text{min}) = 2.68 * 10^{12} * \exp\left(\frac{-66.6}{RT}\right) \sigma^{1.32} \quad (3.14)$$

$$\text{Birthrate, } B^o \text{ (number of crystals/mL.min)} = 8.0 * 10^{16} \exp\left(\frac{-77}{RT}\right) \sigma^{1.5} \quad (3.15)$$

CHAPTER 4

SUCROSE CRYSTALLIZATION

SUCROSE CRYSTALLIZATION

This chapter deals with the study of crystallization of sucrose using CFD. The modeling equations are solved numerically to study the effects of inlet velocity of solution, inlet mass fraction of sucrose and wall temperature of crystallizer on mean crystal diameter and total crystal production.

4.1 Problem Statement

Shiau, 2003 has carried out experimental research on crystallization process. The schematic diagram with proper dimension of the crystallizer used by Shiau, 2003 is shown in figure 4.1. In the present study, the same system is taken up and simulation study is performed to find the effects of inlet velocity, inlet mass fraction of sucrose and wall temperature of crystallizer on the mean crystal diameter and total crystal production using CFD tools. The simulation results are also validated with the Shiau, 2003 experimental data. The commercial software ANSYS Fluent is used for the simulation purpose.

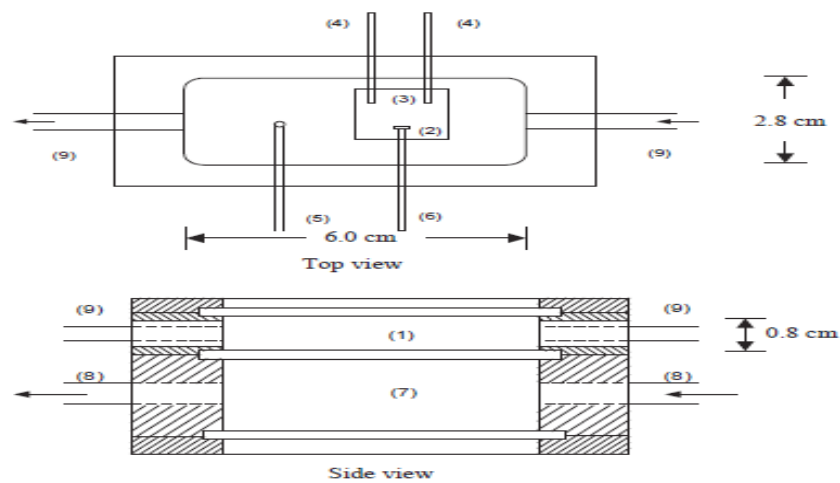


Figure 4.1: Schematic diagram of nucleation cell with the features (Shiau, 2003)

Parts of nucleation cell:

(1) solution chamber, (2) parent crystal, (3) glass cover slip where parent crystal is slid, (4) support rods for glass cover slip (5) thermostat, (6) movable rod holding parent crystal, (7) constant-temperature water chamber, (8) water inlet and outlet, (9) solution inlet and outlet.

In figure 4.1, the rectangular cell has a chamber (1) for crystal nucleation and growth in the upper part and a chamber (7) for temperature-controlled water in the lower part. The rectangular cell was designed for the continuous-flow system in this work. Stimulation is performed in the pure aqueous sucrose solution. A parent crystal (2) was glued to a movable rod (6) and then the growth chamber was injected with the supersaturated sucrose solution. In general, thousands of contact nuclei could be created by sliding the parent crystal along a glass plate (3) in the growth chamber. The glass cover slip is supported by support rod (4) and the thermostat (5) senses the temperature so that the system's temperature is maintained near a desired setpoint. The physical dimensions and operating conditions are listed in table 1.

Table 4.1: Physical dimensions and operating conditions used in simulation.

Parameter	Unit	Range or Value
Length X Width X Height of the crystallizer	m X m X m	0.06 X 0.014 X 0.008
Inlet/Outlet Channel	m X m X m	0.008 X 0.004 X 0.004
Inlet velocity of solution	m/s	0.00001-0.001
Inlet mass fraction of sucrose	Dimensionless	0.70 -0.85
Wall temperature of crystallizer	K	323-333
Inlet temperature of solution	K	303.15

4.2 Geometry and mesh

A 3D geometry of the crystallizer is created in ANSYS workbench and is shown in figure 4.2. Tetrahedral mesh is used for meshing the geometry shown in figure 4.3. It is meshed into 17631 nodes and 47444 elements.

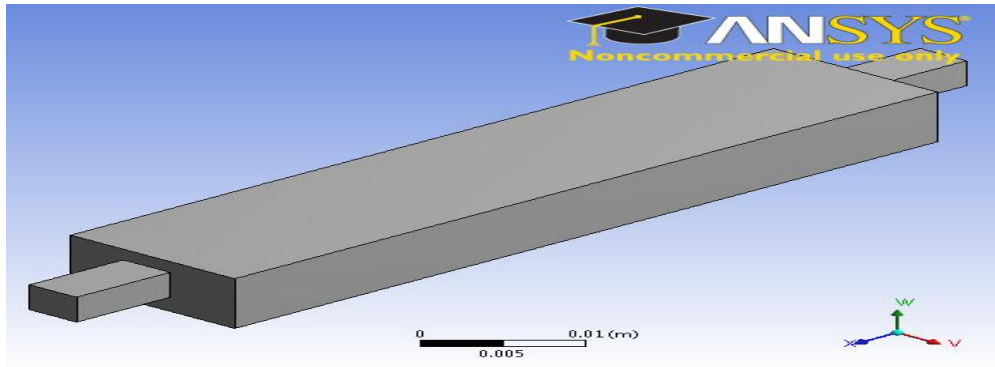


Figure 4.2: Geometry of the crystallizer in ANSYS workbench

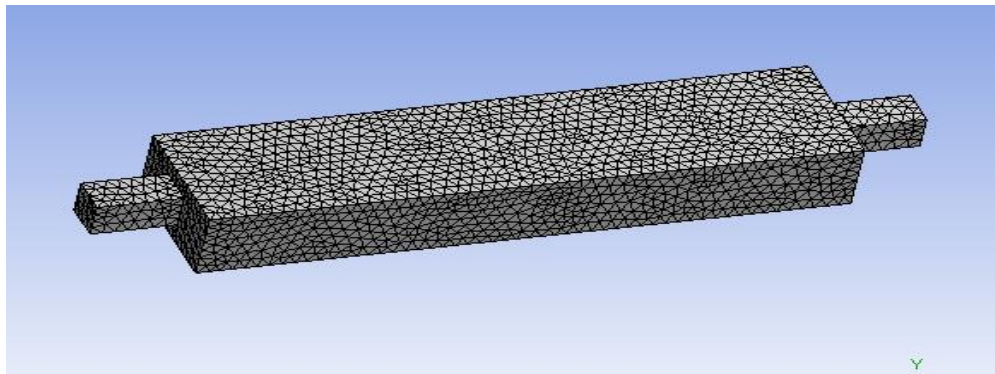


Figure 4.3: Tetrahedral mesh of the crystallizer geometry

4.3 Initial and Boundary conditions, and Solution schemes

Equation 3.1 - 3.15 are solved in the present simulation. In order to obtain a well-posed system of equation, reasonable boundary conditions for the computational domain are implemented. Velocity of the solution, mass fraction of sucrose and temperature of solution are specified at the inlet of the crystallizer. Wall temperature is specified at the wall of the crystallizer and at the outlet pressure boundary condition is specified. No slip boundary condition is specified at the interface of the solid wall and process fluid. In fluent, solver is set as segregated which solves the equation individually. Unsteady state simulation has been formulated. The initial condition for the simulation is 303.15 K, sucrose mass fraction equal to

0.685, stagnant solution and 0.1 nm diameter of the seed in the entire crystallizer. The modeling equations are discretized by the following schemes shown in table 4.2

Table 4.2: Discretization schemes for modeling equations

Equation	Scheme
Momentum	First order upwind
Species Transport for phase-2	First order upwind
Species transport for phase-1	Second order upwind
Volume fraction	Quick Scheme
Gradient	Least square cell method

4.4 Results and discussion

The simulation is carried out to know the variation of local crystal diameter (at position 0.015 m from the inlet) and to calculate the mean crystal diameter in the crystallizer (shown in figure 4.4). The results shows that the mean crystal diameter is more than local crystal diameter up to 240.9s and local crystal diameter is more than mean crystal diameter in between 240-300s. This is obvious because number density of crystals is more in the entire crystallizer than at local position up to 240.9s (shown in figure 4.5) and in between 240-300s the number density of crystals around the local position is more than the entire crystallizer. The initial crystal size is 0.1nm The mean crystal size at 300s is 2.08 μm from simulation and 4.8 μm from experimental (Shiau, 2003). Both the experimental and simulation crystal diameters are of the same order. Therefore CFD models for the crystallizer are validated with the experimental data and hence, the parameter sensitivity on crystallization process can be studied.

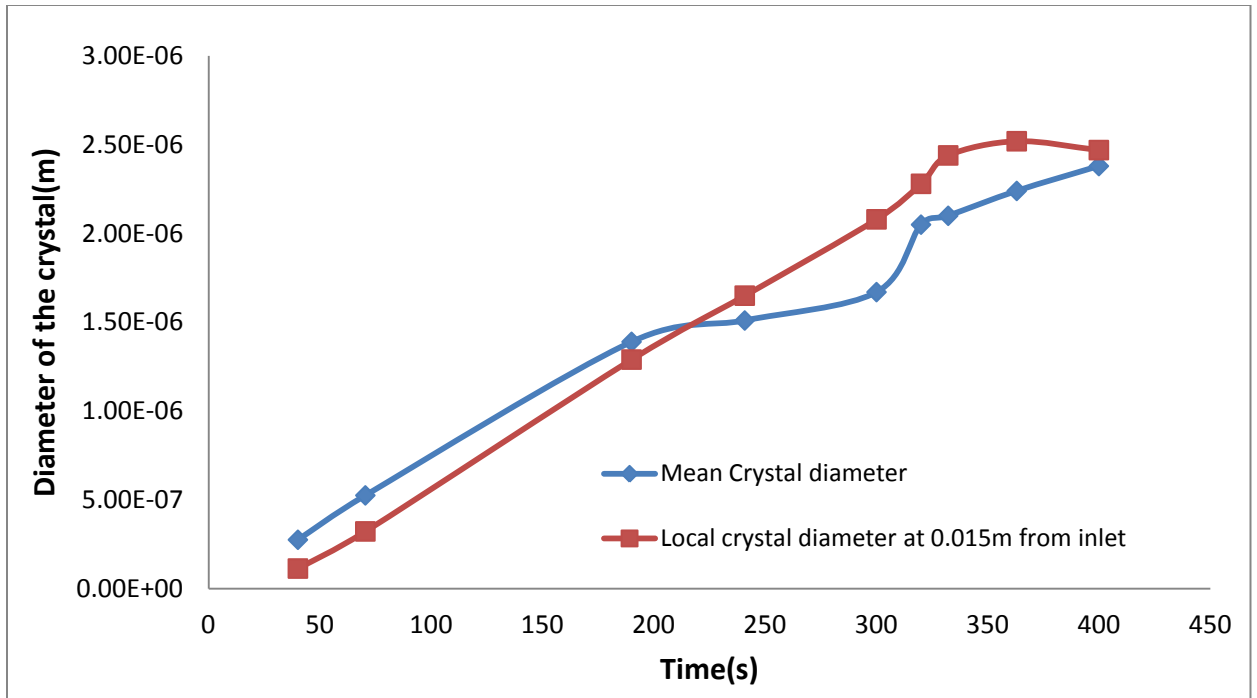


Figure 4.4: Transient distributions of local crystal diameter at location 0.015m from inlet and mean crystal diameter. The used inlet velocity is 0.001067 m/s, inlet mass fraction of sucrose is 0.70 and inlet temperature is 303.15K.

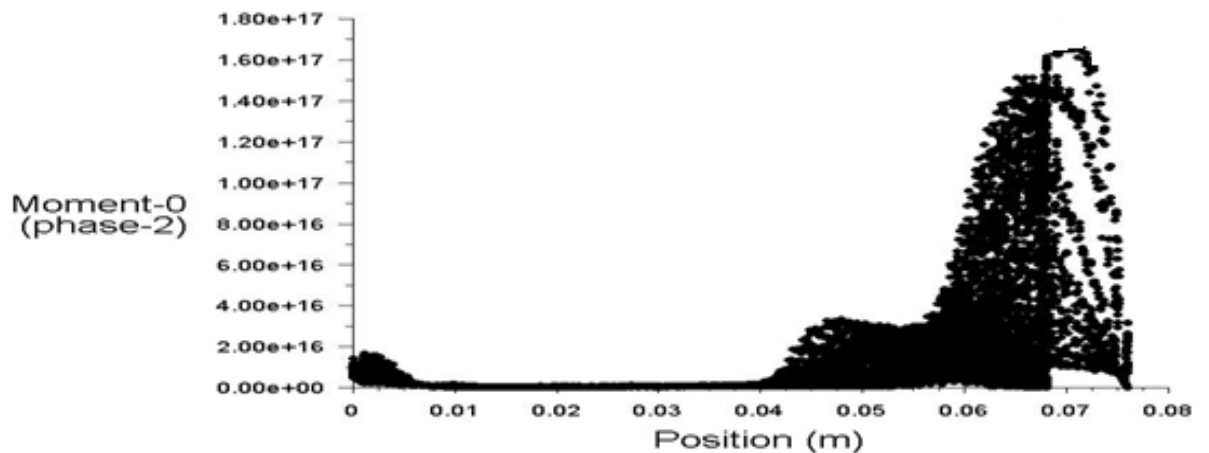


Figure 4.5: Distribution of moment-0 inside the crystallizer at time 240.9 second. The used inlet velocity is 0.001067 m/s, inlet mass fraction of sucrose is 0.70 and inlet temperature is 303.15K. The outlet is present at 0.0 m.

The figure 4.6 shows that the crystal is growing more near the corners of the inlet section where fluid is stagnant as observed through velocity profiles depicted in figure 4.7.

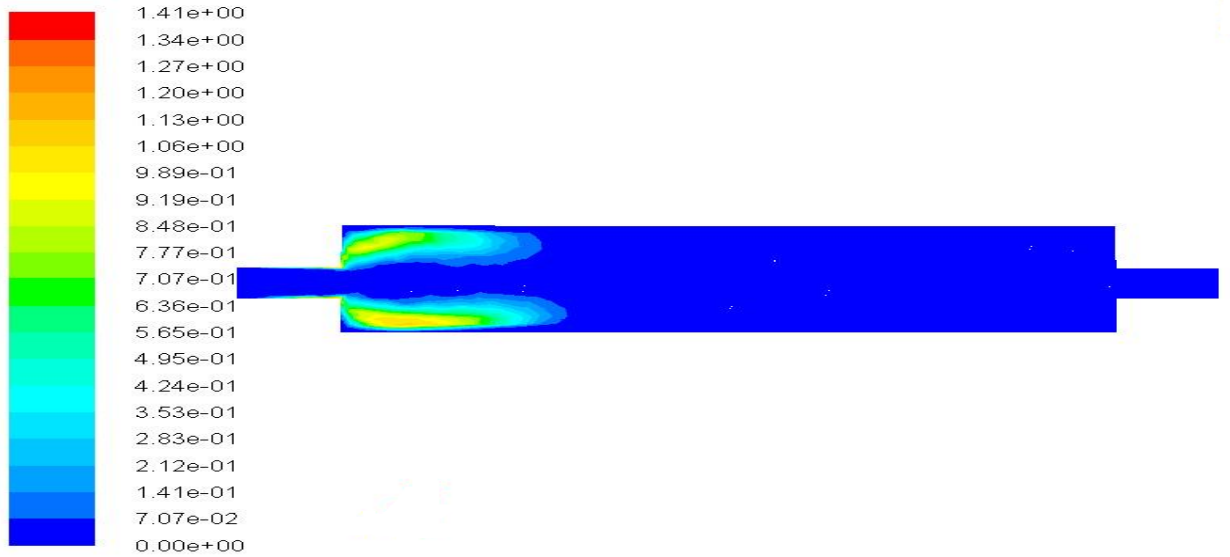


Figure 4.6: Distribution of moment-3 inside the crystallizer at 400 second. The used inlet velocity is 0.001067 m/s, inlet mass fraction of sucrose is 0.70 and inlet temperature is 303.15K. The outlet is present at 0.0 m.

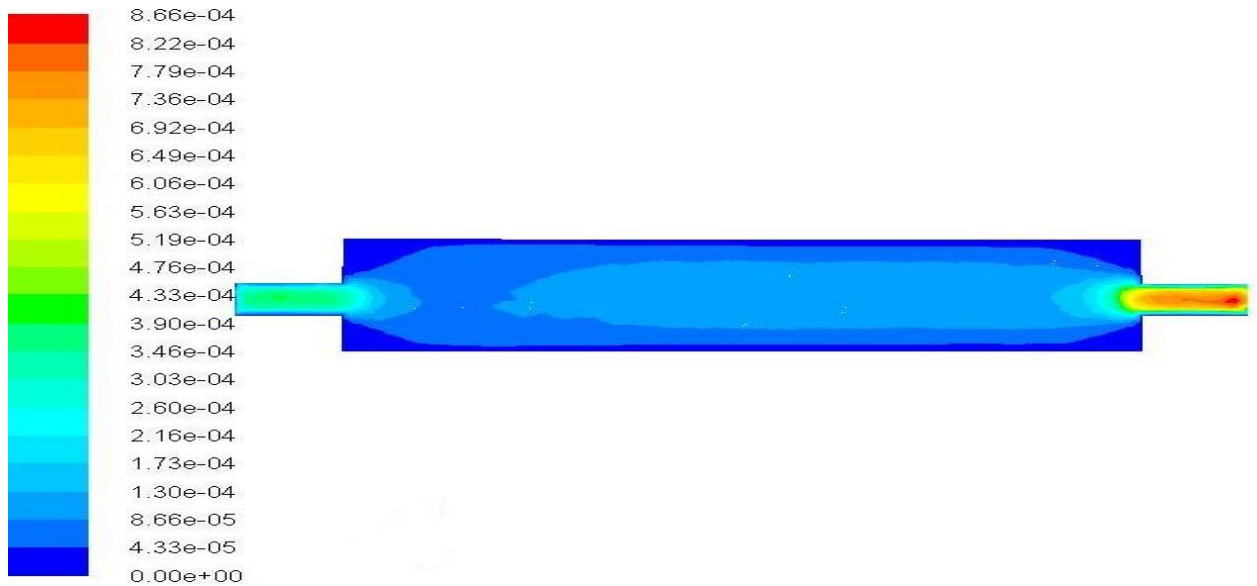


Figure 4.7: Distribution of velocity inside the crystallizer at 400 second. The used inlet velocity is 0.001067 m/s, inlet mass fraction of sucrose is 0.70 and inlet temperature is 303.15K. The outlet is present at 0.0 m.

The study shows population of crystal is more nearer the inlet and hence density of the solution is more at closer to the inlet of the crystallizer than the outlet. It results in increase in velocity at the outlet of the crystallizer found in figure 4.7.

Effect of inlet mass fraction of sucrose on the mean crystal size

The simulation is carried out for a range of inlet mass fraction of sucrose (0.70-0.85) with inlet velocity 0.001067 m/s, initial crystal size 0.1nm and inlet temperature 303.15K. The simulation result as shown in figure 4.8 finds that as the inlet mass fraction of sucrose increases the mean crystal diameter increases upto a certain time and then remains constant except for inlet mass fraction of sucrose 0.70. At higher inlet mass fraction of sucrose, the collisions between the nuclei is increasing, so some nuclei are carried away towards the middle of the crystallizer. The crystal growth is predominant around the middle of the crystallizer (shown in figure 4.9) where the concentration difference is less. This shows that if less concentration difference is present then less number of collisions will occur and the overall displacement due to molecular collision will be towards the crystal surface. After a certain time, around the middle of the crystallizer, the solution is attaining saturation, so crystal growth becomes negligible.

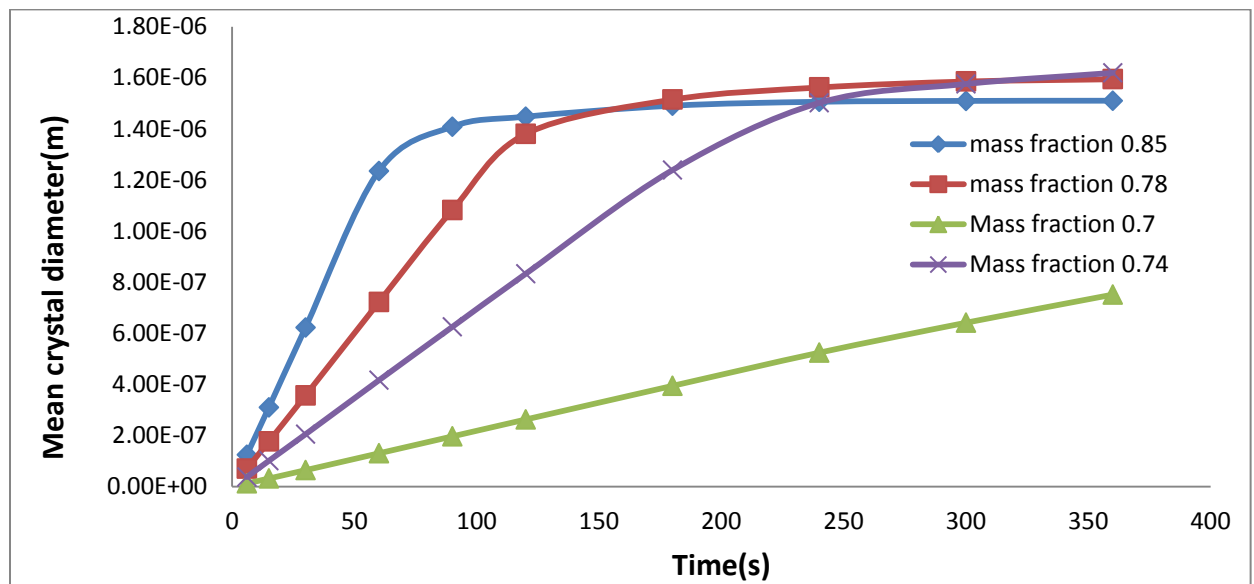


Figure 4.8: Effect of inlet mass fraction of sucrose on the transient distribution of mean crystal diameter. The used inlet velocity is 0.001067 m/s and the inlet temperature is 303.15K.

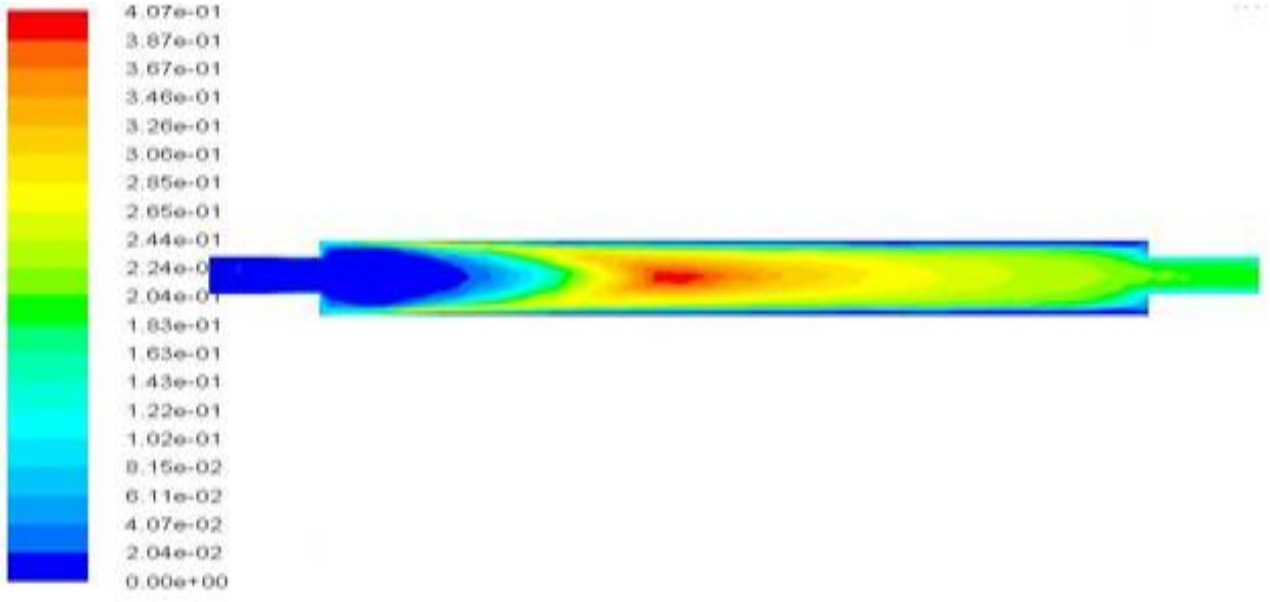


Figure 4.9: Contour plot of moment-3 of the crystallizer at time 360 second. The used inlet velocity is 0.001067 m/s, inlet mass fraction of sucrose is 0.78 and the inlet temperature is 303K. The outlet is present at 0.0 m.

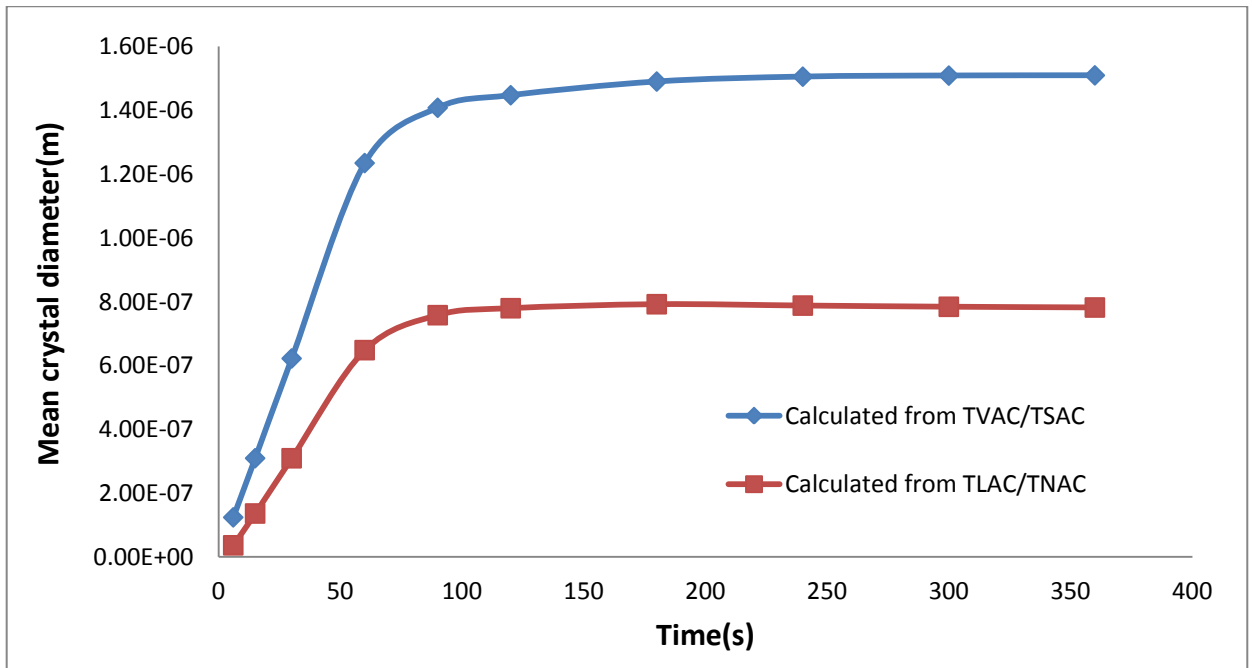


Figure 4.10: Transient distribution of mean crystal diameter obtained by TVAC/TSAC and TLAC/TNAC. The used inlet mass fraction of sucrose is 0.85, the inlet temperature is 303.15K and the inlet velocity is 0.001067 m/s.

The mean crystal diameter is calculated following two methods: (i) by taking the ration of TVAC and TSAC and (ii) by the ratio of TLAC and TNAC. Where, TVAC stands for total volume of all crystals per unit volume of solution (moment 3), TSAC is total surface area of all crystals per unit volume of solution (moment 2), TLAC is total length of all crystals per unit volume of solution (moment 1) and TNAC represents total number of all crystals per unit volume of solution (moment 0).

The stimulation result shown in figure 4.10 is carried out for inlet mass fraction of sucrose 0.85, inlet velocity 0.001067 m/s and inlet temperature 303.15K. There is some difference in results calculated from two methods. But calculation based on TVAC/TSAC gives more accurate results because of consideration of volume shape factor (K_v) and area shape factor (K_a).The simulation result shows that upto 100s the rapid crystal growth size is present and beyond that the crystal size is approximately constant, which happens due to attaining the saturation state.

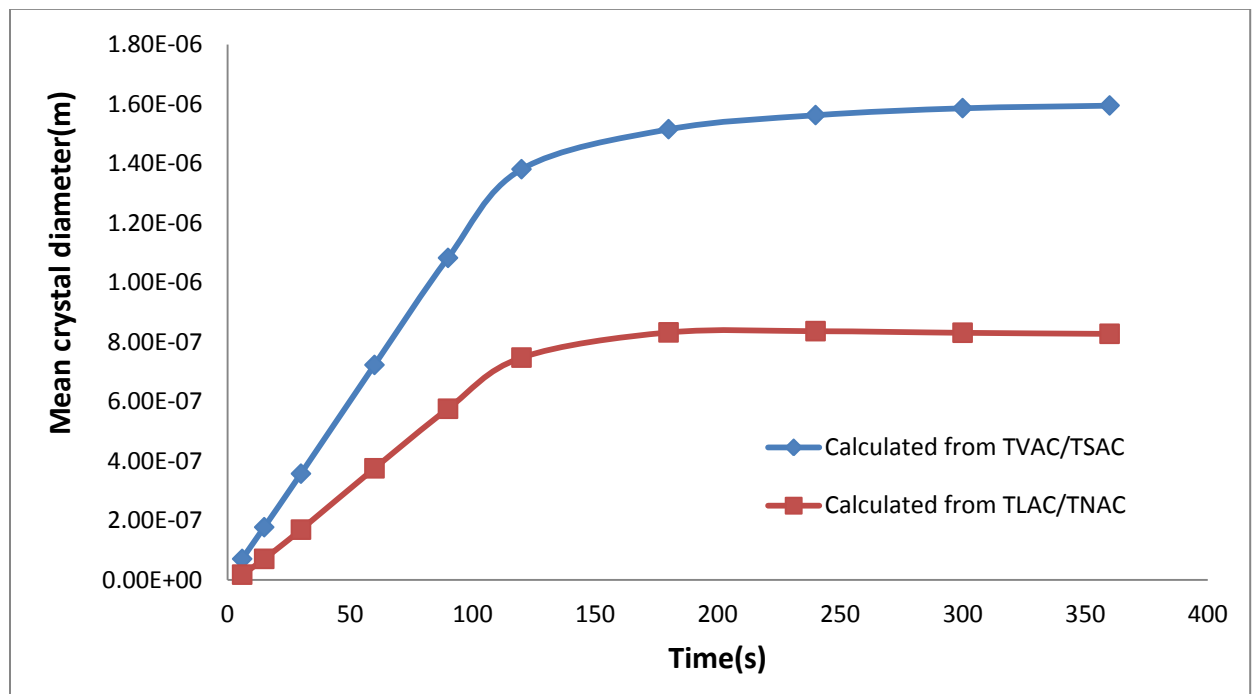


Figure 4.11 Transient distribution of mean crystal diameter obtained by TVAC/TSAC and TLAC/TNAC. The used inlet mass fraction of sucrose is 0.78, the inlet temperature is 303.15K and the inlet velocity is 0.001067 m/s.

The stimulation result shown in figure 4.11 is carried out for inlet mass fraction of sucrose 0.78, inlet velocity 0.001067 m/s and inlet temperature 303.15K. The simulation result shows that upto 110s the rapid crystal growth size is present and beyond that the crystal size is approximately constant. It follows the trend of the figure 4.10 except the increasing trend is shifted by 10 sec more in figure 4.11. It occurs due presence larger concentration gradient at the inlet in the latter case.

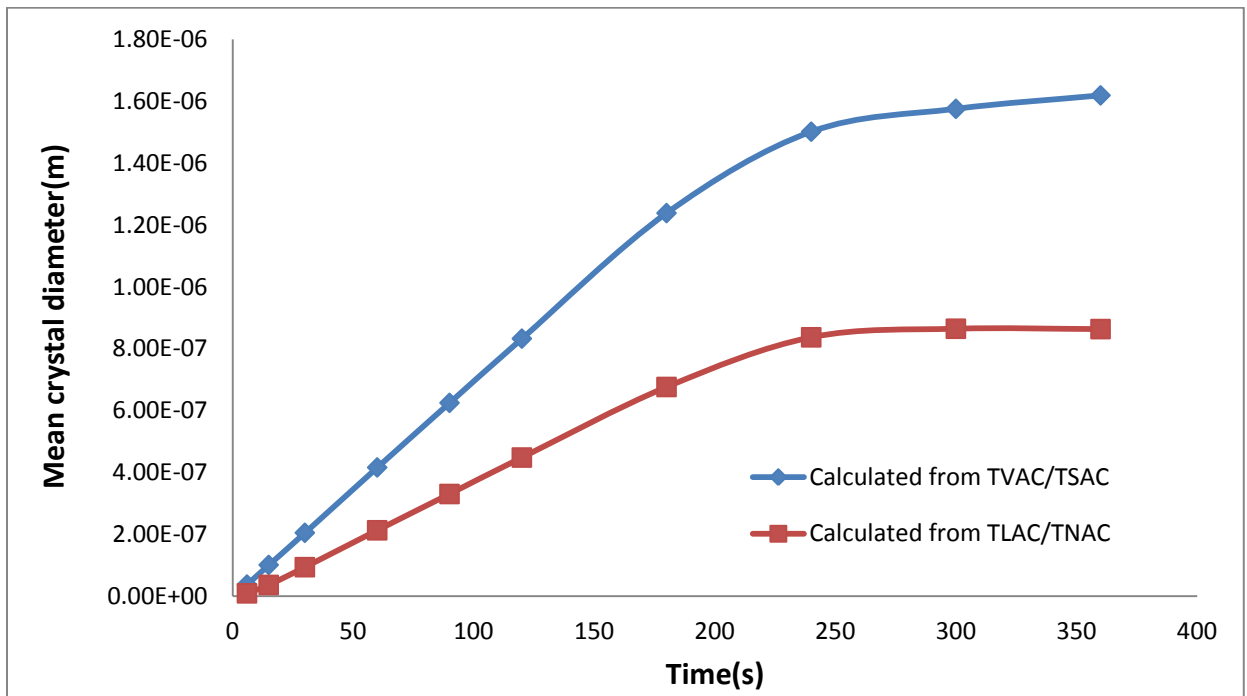


Figure 4.12: Transient distribution of mean crystal diameter obtained by TVAC/TSAC and TLAC/TNAC. The used inlet mass fraction of sucrose is 0.74, the inlet temperature is 303.15K and the inlet velocity is 0.001067 m/s.

The stimulation result shown in figure 4.12 is carried out for inlet mass fraction of sucrose 0.74, inlet velocity 0.001067 m/s and inlet temperature 303.15K. The simulation result shows that upto 200s the rapid crystal growth size is present and beyond that the crystal size is approximately constant. The increasing trend is shifted further in the rightward as compared to figure 4.10 and 4.11 and it follows the same explanation given while comparing figure 4.11 with figure 4.10.

Similarly the simulation result shown in figure 4. 13 is for same operating conditions but inlet mass fraction is 0.7. The mean crystal diameter is increasing linearly with time for low degree of supersaturation and crystal started growing near the inlet corners of the crystallizer. The crystallization process at low supersaturation is advisable as strong crystals and non-agglomerating crystals can be formed and the more volume of the crystallizer can be utilized for crystal growth.

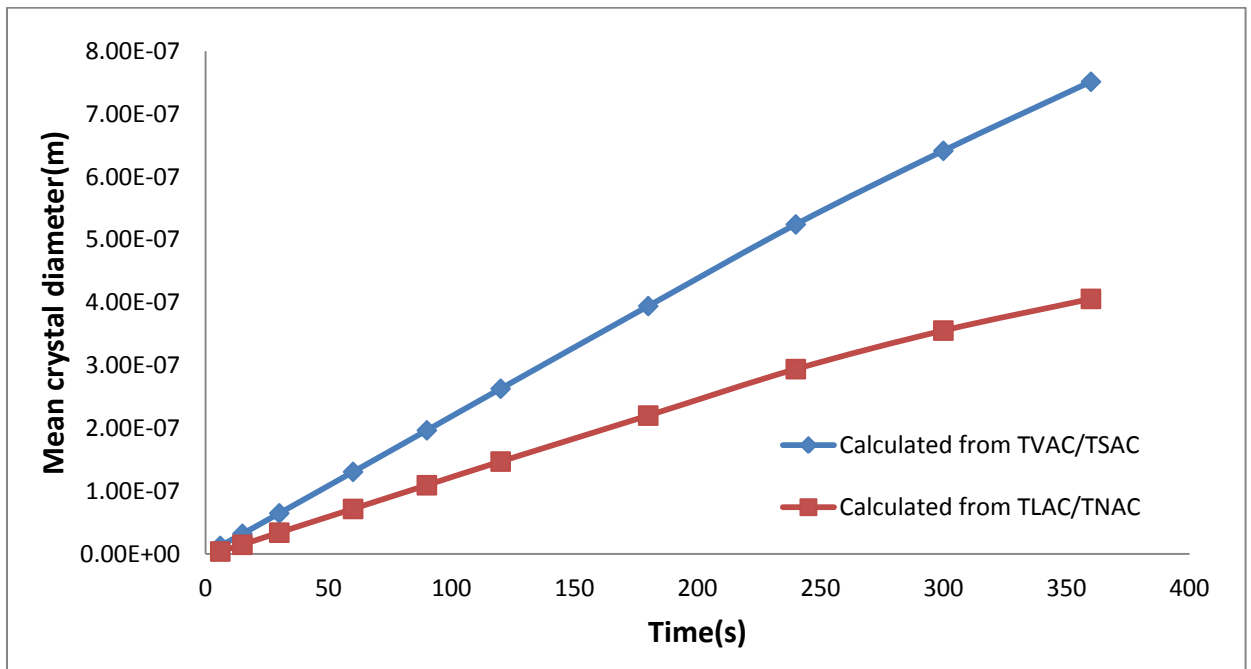


Figure 4.13: Transient distribution of mean crystal diameter obtained by TVAC/TSAC and TLAC/TNAC. The used inlet mass fraction of sucrose is 0.70, the inlet temperature is 303.15K and the inlet velocity is 0.001067 m/s.

Effect of inlet mass fraction of sucrose on total crystal production

The simulation is carried out for a range of inlet mass fraction of sucrose (0.7-0.85), inlet velocity 0.001067 m/s, initial crystal size 0.1nm and inlet temperature 303.15K shown in figure 4.14. The simulation result as shown in figure 4.14 finds that as the inlet mass fraction of sucrose increases the number density increases upto a certain time and then remains constant except for inlet mass fraction of sucrose 0.70. This shows that after certain time the system is attaining dynamic equilibrium and the system will attain dynamic equilibrium quickly for high

inlet mass fraction of sucrose. As the concentration increases the molecular collisions between the nuclei increases and the mean crystal diameter will be less. Also at larger supersaturation the crystal growth is characterized by abnormal needlelike or whisker like growth from the ends of the crystals, which, under these conditions, may grow much faster than the sides. The spikes are imperfect crystals which are bound to the parent crystal by weak forces and which break off to give crystals of poor quality. At higher mass fraction of sucrose the mother liquor may be occluded between crystals during crystal growth. So loosely bonded crystals will be formed which may dissociate into individual particles. The simulation results also shows that at low supersaturation a linear increase in number density is observed which is helpful for controlling the crystallization process.

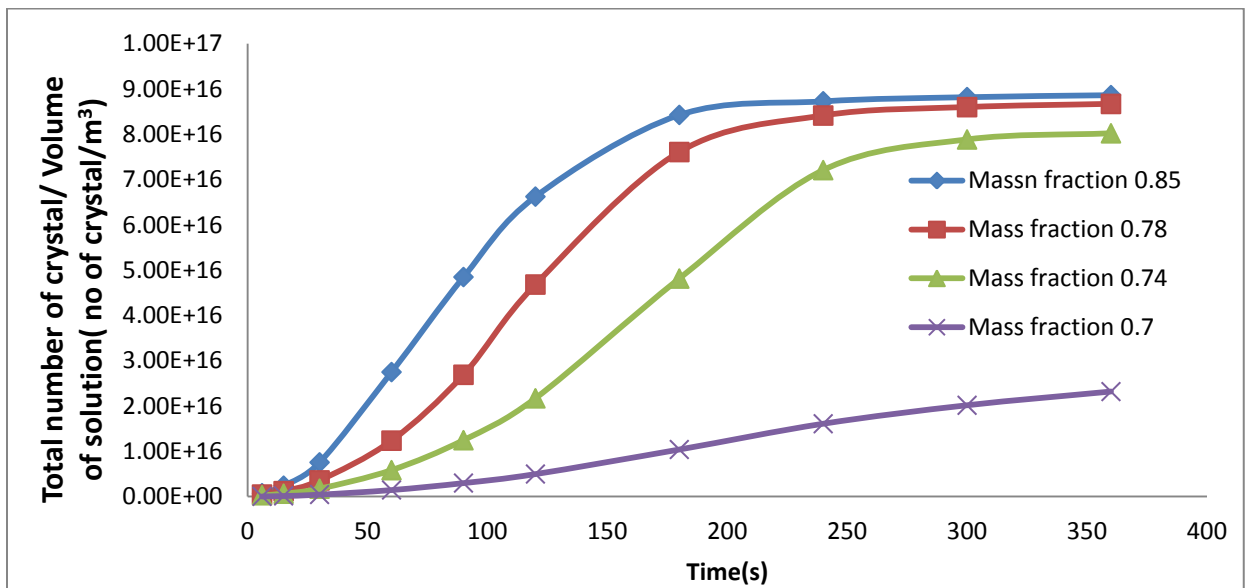


Figure 4.14: Effect of inlet mass fraction of sucrose on the transient distribution of number density of the crystallizer. The used inlet velocity of solution is 0.001067 m/s and the inlet temperature is 303.15K individually.

Effect of inlet velocity of solution on mean crystal size

The simulation is carried out for a range of inlet velocity (0.00001-0.001m/s), inlet mass fraction of sucrose 0.70, initial crystal size 0.1nm and inlet temperature 303.15K (shown in figure 4.15). In a supersaturated solution the mass transfer of solute takes place from low

concentration zone to high concentration zone of it. The crystal growth is two step processes. Formerly the mass transfer of nuclei towards the crystal surface and latter is surface reaction on the crystal surface. The results show that with decrease in velocity the mean crystal diameter is increasing. This shows that at higher velocities of solution, the velocity of fluid is dominating the mass transfer rate, so majority of the nuclei are carried away from the crystal surface.

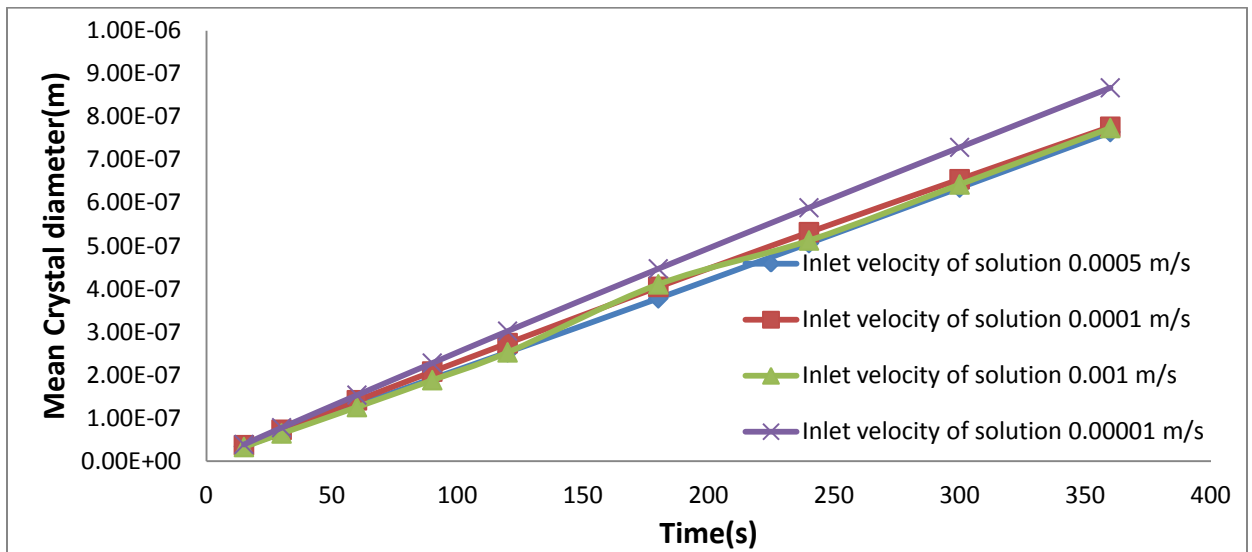


Figure 4.15: Effect of the inlet velocity on the transient distribution of mean crystal diameter inside the crystallizer. The used inlet mass fraction of sucrose is 0.70 and the inlet temperature is 303.15K.

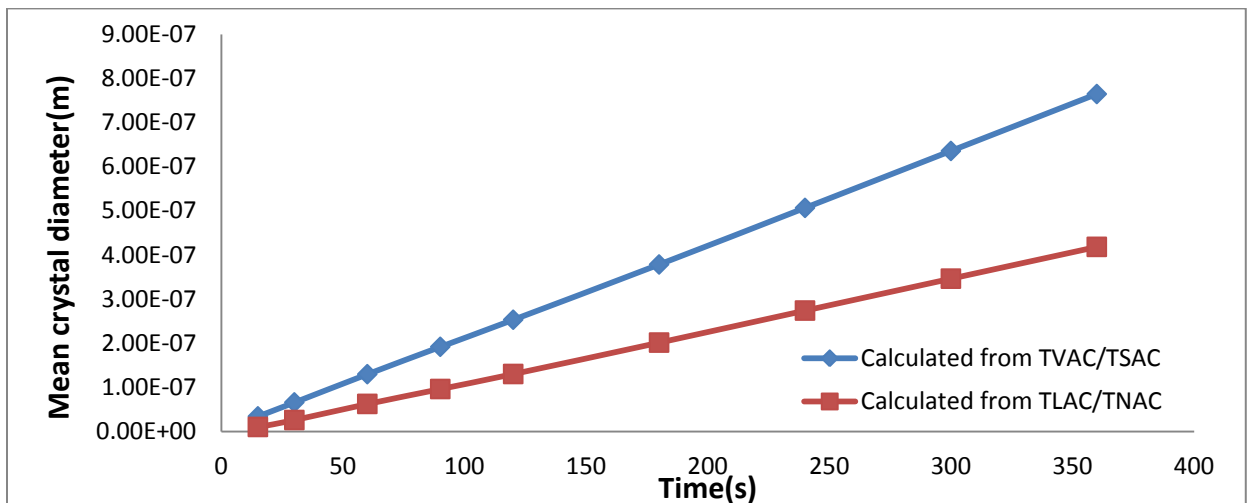


Figure 4.16: Transient distribution of mean crystal diameter obtained by TVAC/TSAC and TLAC/TNAC. The used inlet mass fraction of sucrose is 0.70, the inlet temperature is 303.15K and the inlet velocity is 0.0005 m/s.

The simulation shown in figure 4.16 is for inlet mass fraction of sucrose 0.70, inlet velocity 0.0005m/s, initial seed crystal size 0.1nm and inlet temperature 303.15K. The mean crystal diameter can be calculated by two methods, one is by ratio of moment-3 to moment-2 and the other is by ratio of moment-1 to moment-0. The former one is more accurate as volume shape factor and area shape factor is taken into consideration. The simulation result finds that the mean crystal size is increasing linearly with time. The mean crystal diameter for velocity 0.0005m/s is more than the mean crystal size for velocity 0.001m/s and less than the mean crystal size for velocity 0.0001m/s and 0.00001m/s. This shows the mean crystal size increases with decrease in inlet velocity. Also the number density for velocity, 0.0005m/s is more than number density for inlet velocity, 0.001m/s. This shows at high velocity because of velocity current the nuclei are carried away from the crystal surface instead of towards the crystal surface.

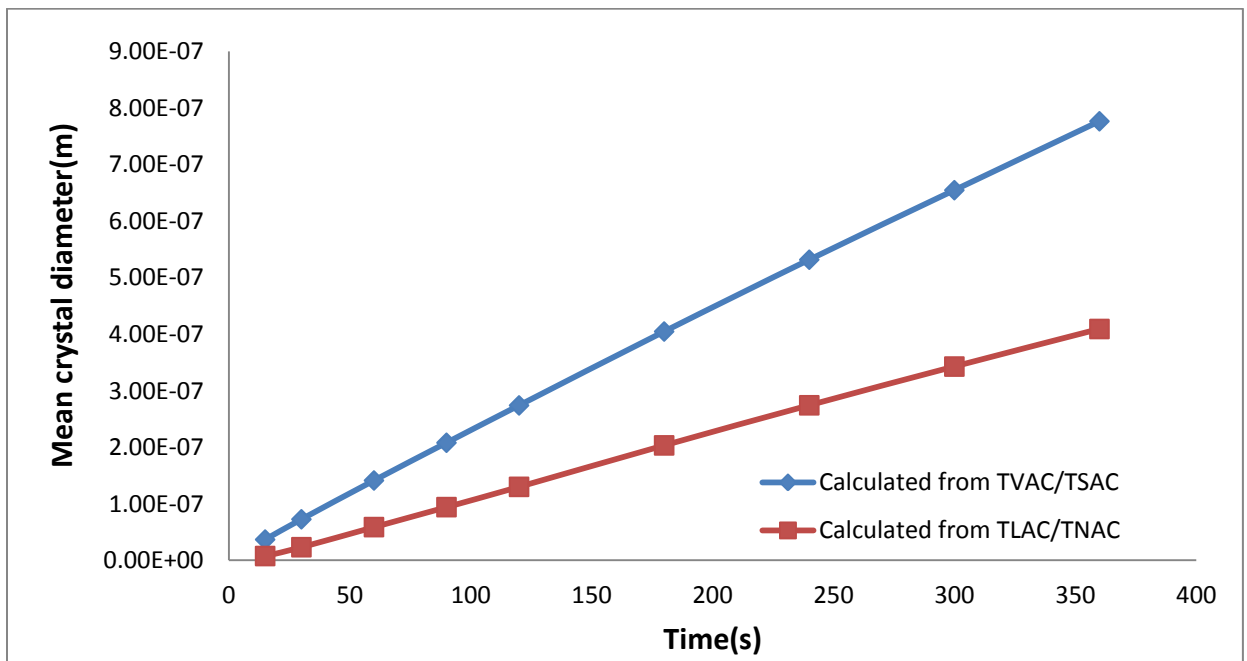


Figure 4.17: Transient distribution of mean crystal diameter obtained by TVAC/TSAC and TLAC/TNAC. The used inlet mass fraction of sucrose is 0.70, the inlet temperature is 303.15K and the inlet velocity is 0.0001 m/s.

The simulation shown in figure 4.17 is for inlet mass fraction of sucrose 0.70, inlet velocity 0.0001m/s, initial seed crystal size is taken as 0.1nm and inlet temperature

303.15K. The simulation results show that the mean crystal size is increasing linearly with time. The mean crystal diameter for velocity 0.0001m/s is more than the mean crystal size for velocity 0.0005m/s, 0.001m/s and less than the mean crystal size for velocity 0.00001m/s. This shows the mean crystal size increases with decrease in inlet velocity of solution. Also the number density for velocity of solution 0.0001m/s is more than number density for inlet velocity of solution 0.0005m/s and 0.001m/s. This shows at higher inlet velocity of solution because of velocity current the nuclei are carried away from the crystal surface instead of towards the crystal surface.

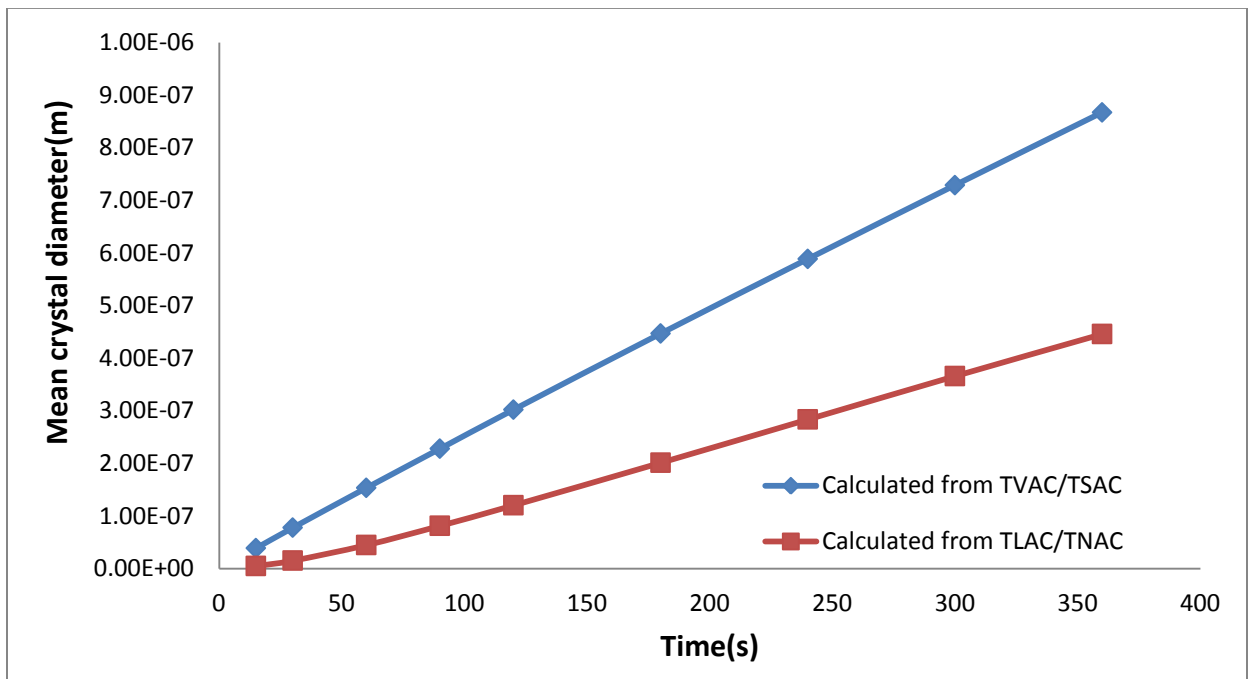


Figure 4.18: Transient distribution of mean crystal diameter obtained by TVAC/TSAC and TLAC/TNAC. The used inlet mass fraction of sucrose is 0.70, the inlet temperature is 303.15K and the inlet velocity is 0.00001 m/s.

Similarly the simulation is carried out for same operating conditions but for different inlet velocity 0.00001m/s (shown in figure 4.18) and 0.001m/s (shown in figure 4.19) and for both the inlet velocities, the mean crystal size is increasing linearly with time. The simulation result shows that the mean crystal size is more for less inlet velocity of solution. The number density present in the solution is lowest for the least inlet velocity of solution. This shows at lower inlet

velocity of solution the mass transfer rate is dominating than the velocity current and the nuclei are carried toward the crystal surface.

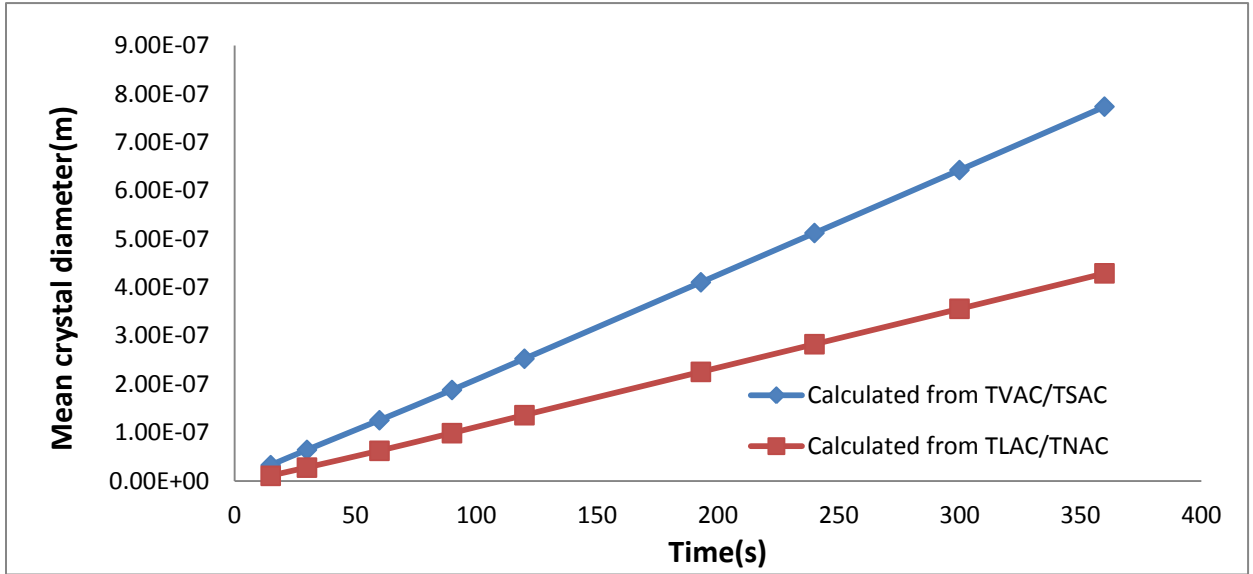


Figure 4.19: Transient distribution of mean crystal diameter obtained by TVAC/TSAC and TLAC/TNAC. The used inlet mass fraction of sucrose is 0.70, the inlet temperature is 303.15K and the inlet velocity is 0.001 m/s.

Effect of inlet velocity of solution on total crystal production

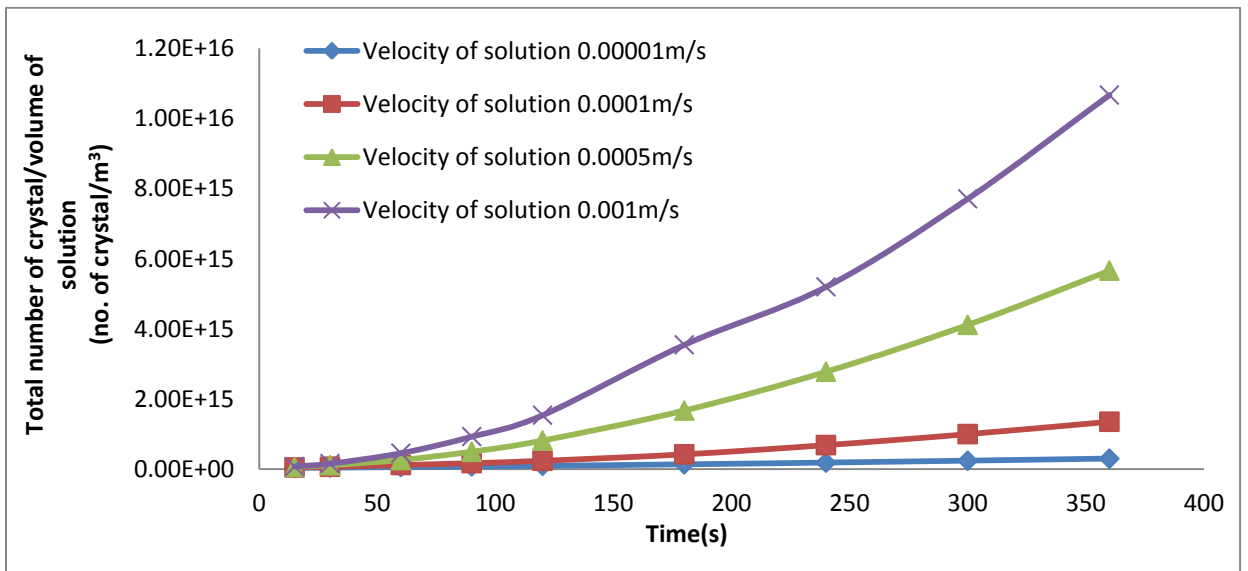


Figure 4.20: Effect of inlet velocity on the transient distribution of number density of crystals. The used inlet mass fraction of sucrose is 0.70 and the inlet temperature is 303.15K

The simulation result shown in figure 4.20 is carried out for different inlet velocity (0.00001m/s- 0.001m/s), for inlet mass fraction of sucrose 0.70 and for initial crystal size 0.1nm and inlet temperature 303.15K. The simulation result shows that as the inlet velocity of solution is decreasing, the number density is decreasing. This shows that at lower inlet velocity of solution the nuclei is transferred towards the crystal surface and mean crystal size is increasing shown in figure 4.14.

Effect of temperature of wall on total crystal production

There is no effect of wall temperature on the mean crystal diameter (shown in figure 4.22) but the production of crystals is increasing (shown in figure 4.21) with increase in wall temperature. The simulation shows that the solution is attaining saturation around 180s because of wall temperatures. The crystal growth is more in the zone where the temperature is less and the crystal growth is less in the zone where the temperature is more (shown in figure 4.25). This shows that with increase in temperature the molecular collision is increasing and the nuclei are not agglomerating.

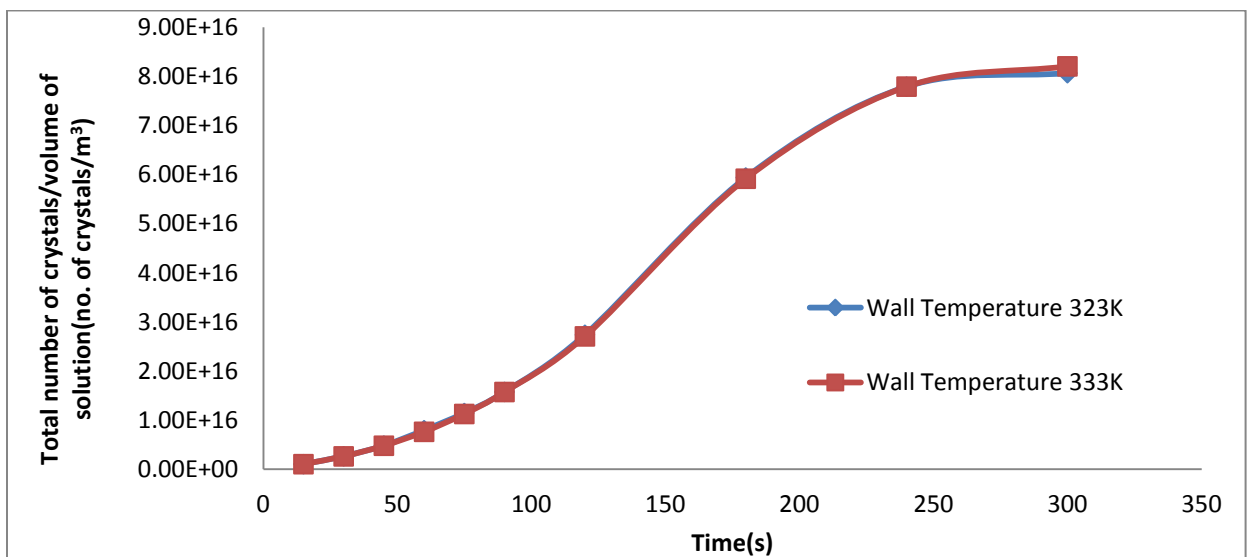


Figure 4.21: Effect of the wall temperature of the crystallizer on the transient distribution of number density of the crystals inside the crystallizer. The used inlet mass fraction of sucrose is 0.7, the inlet temperature is 303.15 K and the inlet velocity is 0.001m/s.

Effect of temperature of wall on mean crystal size

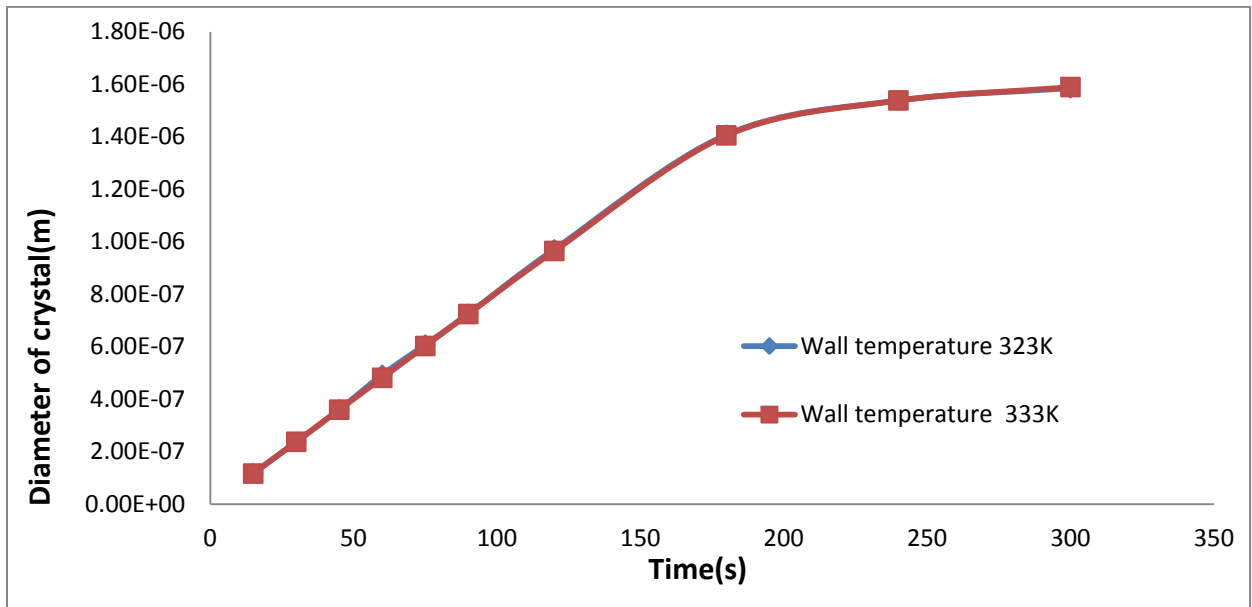


Figure 4.22: Effect of the wall temperature of the crystallizer on the transient distribution of mean crystal diameter. The used inlet mass fraction of sucrose is 0.70, the inlet temperature is 303.15 K and the inlet velocity is 0.001 m/s.

The simulation result for a range of wall temperatures (323K, 333K), inlet velocity 0.001067 m/s, initial seed crystal size 0.1 nm and inlet mass fraction of sucrose 0.70 and inlet temperature 303.15 K. The crystal size is increasing linearly with time up to 180 s and then the crystal size is nearly constant. But for isothermal system shown in figure 4.23 the supersaturation is prevailing for at least 360 s. This shows that desupersaturation is taking place from 180 s onwards because of wall temperature.

The simulation shown in figure 4.23 is for inlet velocity 0.001067 m/s, inlet mass fraction 0.70, wall temperature 323K, initial seed crystal size 0.1 nm, inlet temperature 303.15 K and wall temperature of crystallizer 323K. The mean crystal diameter can be calculated by two methods, one is by ratio of moment 3 to moment 2 and the other is by ratio of moment 1 to moment 0. The former one is more accurate as volume shape factor and area shape factor is taken into consideration. The mean crystal size is increasing up to 180 s and beyond 180 s onwards there is no change in crystal size. This shows the supersaturation is prevailing up to 180 s and beyond the

solution is saturated. Similarly for figure 4.24 but wall temperature of crystallizer is 333K and the system is attaining equilibrium just 178s (approximately)

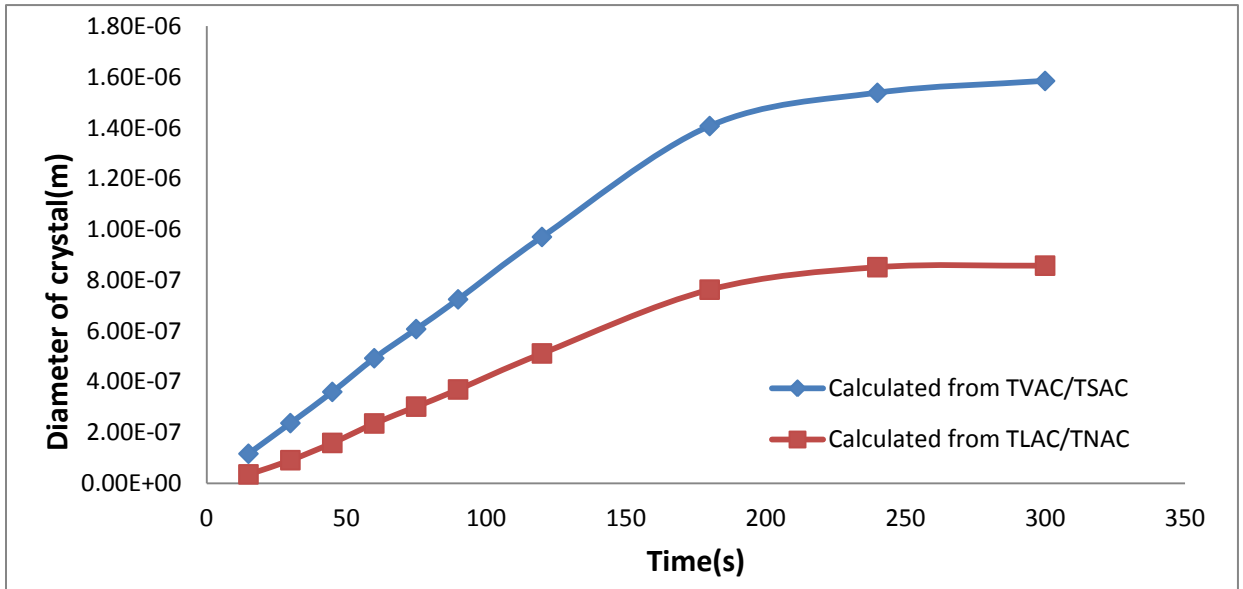


Figure 4.23: Transient distribution of mean crystal diameter obtained by TVAC/TSAC and TLAC/TNAC. The used inlet mass fraction of sucrose is 0.70, the inlet temperature is 303.15K and the inlet velocity is 0.001067 m/s. The specified wall temperature is 323 K

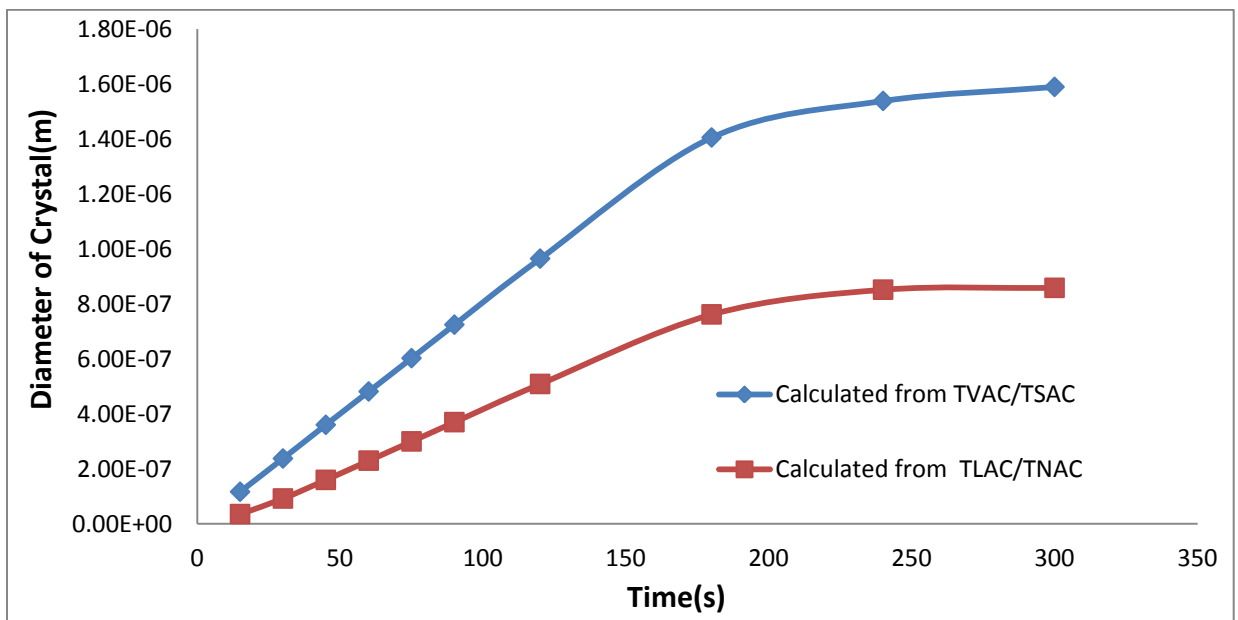


Figure 4.24: Transient distribution of mean crystal diameter obtained by TVAC/TSAC and TLAC/TNAC. The used inlet mass fraction of sucrose is 0.70, the inlet temperature is 303.15K and the inlet velocity is 0.001067 m/s. The specified wall temperature is 333 K.

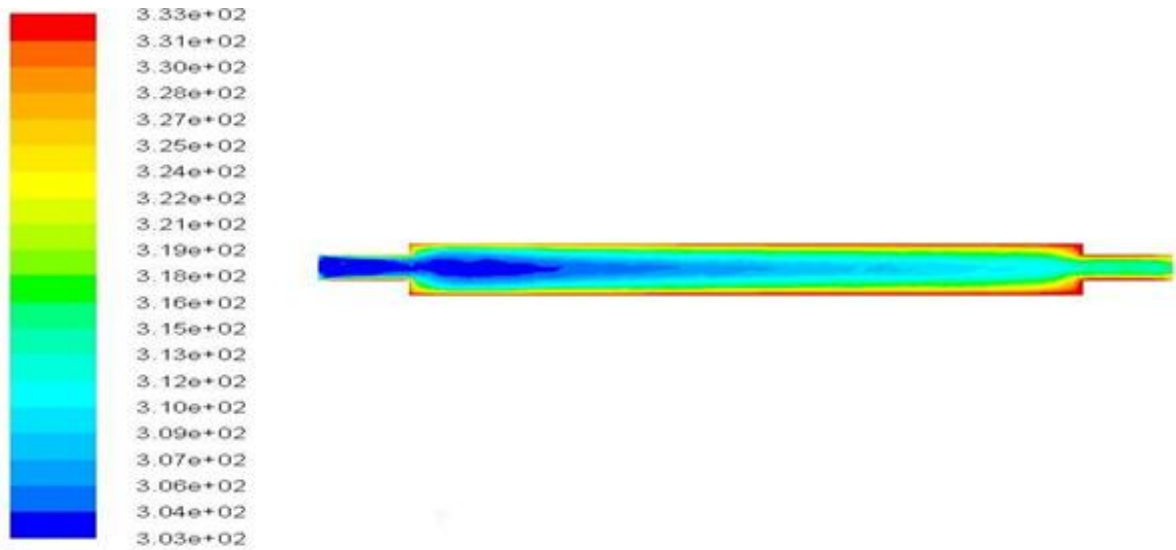


Figure 4.25: Contour plot of the temperature of the crystallizer at time 300second. The used inlet velocity of is 0.001067 m/s, inlet mass fraction of sucrose is 0.70 and the inlet temperature is 303.15K. The specified wall temperature is 333 K. The outlet is present at 0.0 m.

The counter plot showed in figure 4.24 and figure 4.25 shows that the crystals are growing around the middle region of the crystallizer where the temperature is less or in the region where the wall temperature effect is negligible. This shows that as the temperature increases the collision increases.

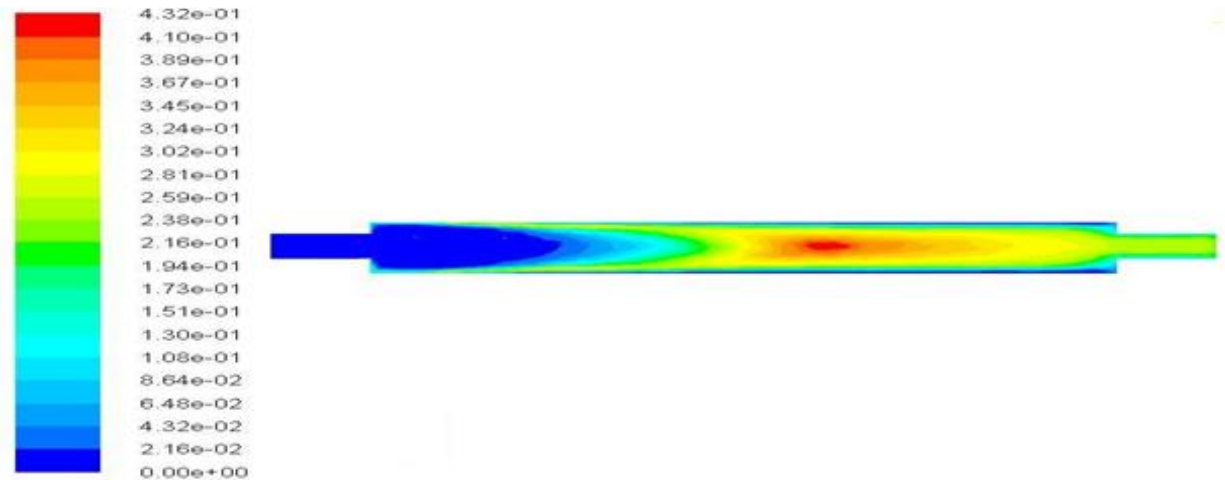


Figure 4.26: Contour plot of moment-3 of the crystallizer at time 300second. The used inlet velocity is 0.001067 m/s, inlet mass fraction of sucrose is 0.70 and the inlet temperature is 303.15K. The specified wall temperature is 333 K. The outlet is present at 0.0 m.

CHAPTER 5

CONCLUSION

CHAPTER 5**CONCLUSION**

CFD analysis of sucrose crystallization is carried out using transient simulations in a continuous flow chamber. From the rigorous study the followings can be concluded.

- ✓ CFD results were able to capture the experimental results with satisfaction.
- ✓ The time dependent mean crystal diameter depends on the inlet mass fraction of sucrose. With increase in the inlet mass fraction of sucrose the mean crystal diameter was increased up to certain time and then it becomes constant.
- ✓ The total crystal production or crystal number density was found to be increased with increase in inlet mass fraction of sucrose
- ✓ The time dependent mean crystal diameter was found to depend on the inlet velocity and with decrease in velocity the mean crystal diameter was increased.
- ✓ The total crystal production was found to be increased with increase in inlet velocity of solution.
- ✓ The production of crystals was increased with increase of wall temperature but mean crystal diameter was found invariant with wall temperature.

FUTURE SCOPE

In future experimental work can be carried out to find out the effect of inlet mass fraction of sucrose, inlet velocity and temperature and wall temperatures of the crystallizer on the crystallizer performance. The simulated data in the present study can be compared with these experimental data for better designing of the crystallizer.

REFERENCES

1. Abbas, A. and Romagnoli, J., “Multiscale modeling, simulation and validation of batch cooling crystallization”, *Separation and Purification Technology*, 2006, 153-163.
2. Abdel, N., Mohameed, H., Nasr, A. and Takrouri, K., “Model-based optimal cooling strategy for batch crystallization processes”, *Chemical Engineering Research and Design*, 2003, 35-46.
3. Albert, M. and Allan, S., “Handbook of industrial crystallization”, 1993, 2nd edition, 38-120.
4. Andre, B., Everson, A. and Gisele, A., “Determination of crystal growth rate for porcine insulin crystallization with CO₂ as a volatile acidifying agent”, *Chemical Engineering and Processing: Process Intensification*, 2012, 29– 33.
5. Angelov, I., Ashfaq, A., Elsner, M., Seidel-Morgenstern, A., Qamara, S. and Warnecke, G., “Adaptive high-resolution schemes for multidimensional population balances in crystallization processes”, *Computers & Chemical Engineering*, 2007, 1296–1311.
6. Angelov, I., Ashfaq, A., Elsner, M., Seidel-Morgenstern, A., Qamara, S. and Warnecke, G., “A comparative study of high resolution schemes for solving population balances in crystallization”, *Computers & Chemical Engineering*, 2006, 1119–1131.
7. Angelov, I., Ashfaq, A., Elsner, M., Seidel-Morgenstern, A., Qamara, S. and Warnecke, G., “Numerical approximations of a population balance model for coupled batch preferential crystallizers”, *Applied Numerical Mathematics*, 2009, 739–753.
8. ANSYS Fluent 13.0 Theory Guide, 2009.
9. Basim, A., Hazim, A. and Mohamad, K., “Effect of cooling rate on unseeded batch crystallization of KCl”, *Chemical Engineering and Processing: Process Intensification*, 2002, 297–302.
10. Benedito, J., Corona, E., Garcia-Perez, J. and Santacatalina, J., “Ultrasonic monitoring of lard crystallization during storage”, *Food Research International*, 2011, 146-155.

11. Bento, L., Ferreira, A., Khaddour, I. and Rocha, F., "Kinetics and thermodynamics of sucrose crystallization from pure solution at different initial supersaturations", *Surface Science*, 2010, 1208–1214.
12. Chirag, M. and Damien, J., "Nucleation and growth kinetics of struvite crystallization", *Water Research*, 2013, 2890–2897.
13. Daniele, L., Jay, S., Kumar, D. and Rodney, O., "On the comparison between population balance models for CFD simulation of bubble columns", *Industrial and Engineering Chemistry Research*, 2005, 5063–5072.
14. Darmont, J. and Detry, L., "Process and equipment for crystallizing and inorganic substance", 1992, U.S. Patent.
15. David, R., Muhw, H. and Villermaux, J., "Solving population balance in the case of the precipitation of silver bromide crystals with high primary nucleation rates by using the first order upwind differentiation", *Chemical Engineering Science*, 1996, 309–319.
16. En, S., Gibaek, L., Jean, M., Xavier, J., Xuan, M. and Young, L., "On the solution of population balance equations (PBE) with accurate front tracking methods in practical crystallization processes", 2009, *Chemical Engineering Science*, 3715 – 3732.
17. Espinosa, R., Franke, L. and Deckelmann, G., "Model for the mechanical stress due to the salt crystallization in porous materials", *Construction and Building Materials*, 2007, 1350–1367.
18. Fevotte, G., Klein, J. and Puel, F., "Simulation and analysis of industrial crystallization processes through multidimensional population balance equations", *Chemical Engineering Science*, 2003, 3729–3740.
19. Garside, J., Mullin, J. and Das, S., "Growth and dissolution kinetics of potassium sulfate crystals in an agitated vessel", *Industrial and Engineering Chemistry Research*, 1974, 299–301.
20. Gerald, W. and Shamsul, Q., "Numerical solution of population balance equations for nucleation, growth and aggregation processes", *Computers & Chemical Engineering*, 1996, 1576–1589.
21. Gerald, W. and Shamsul, Q., "Solving population balance equations for two-component aggregation by a finite volume scheme", *Chemical Engineering Science*, 2007, 679 – 693.

22. Gilles, D., Mitrovi, A. and Motz, S., "Comparison of numerical methods for the simulation of dispersed phase systems", *Chemical Engineering Science*, 2002, 4329 – 4344.
23. Guo, Z., Jones, G. and Li, N., "The effect of ultrasound on the homogeneous nucleation of BaSO₄ during reactive crystallization", *Journal of Applied Physics*, 2006, 1617 – 1626.
24. Hairong, L., Hong, L., Yu, L. and Zhichao, G., "The application of power ultrasound to reaction crystallization", *Ultrasonics Sonochemistry*, 2006, 359-363.
25. Heinrich, S., Kumar, J., Peglow, M. and Warnecke, G., "Comparison of numerical methods for solving population balance equations incorporating aggregation and breakage", *Powder Technology*, 2009, 218–229.
26. Hussain, S., Lionberger, A., Raw, S., D'Costa, R., Wu H. and Yu, X., "Applications of process analytical technology to crystallization processes", *Advanced Drug Delivery Reviews*, 2004, 349–369.
27. Jonathan, A. and Mikael, A., "CFD modeling of sucrose crystallization", 1999, Second International Conference, Australia, 381-386.
28. Jones, G., "Crystallization process systems", 2002, 2nd edition, 60-140.
29. Jones, G., Kougoulos, E. and Narducci, O., "Continuous crystallization of adipic acid with ultrasound", *Chemical Engineering Science*, 2011, 1069-1076.
30. Julian, C., Peter, H. and Warren, L., "Unit operations of chemical engineering" 5th edition, 882-901.
31. Keisuke, F., Kouji, M., Yuichi, Y. and Yusuke, A., "Determination of crystal nucleus size of potassium chloride from ethanol solution caused by ultrasonic irradiation", *Chemical Engineering and Processing: Process Intensification*, 2009, 902–906.
32. Kordylla, A., Krawczyk, T., Schembecker, G. and Tumakaka, F., "Modeling ultrasound-induced nucleation during cooling crystallization", *Chemical Engineering Science*, 2009, 1635 -1642.
33. Lawrence, E. and Verdoes, D., "Process and equipment for carrying out crystallization", 2007, U.S. Patent.
34. Lindberg, M. and Rasmuson, C., "Reaction crystallization in strained fluid films", *Chemical Engineering Science*, 2000, 3257-3273.
35. Mullin, J., "Crystallization", 1993, 3rd edition, 20-80.

36. Ramkrishna, D. and Sanjeev, K., “On the solution of population balance equations by discretization-III nucleation, growth and aggregation of particles”, *Chemical Engineering Science*, 1997, 4659- 4679.
37. Reginald, B., Richard, D. and Xing, Y., “Modeling and computational fluid dynamics-population balance equation-micromixing simulation of impinging jet crystallizers”, *Crystal Growth and Design*, 2009, 1156–1164.
38. Rohani, S., “Nucleation, growth, and aggregation kinetics of potassium chloride from a continuous mixed-suspension mixed product removal cooling crystallizer”, *Separations Technology*, 1993, 99-105.
39. Saxer, K., “Fractional crystallization process”, 1984, U.S. Patent.
40. Shiau, D., “The distribution of dislocation activities among crystals in sucrose crystallization”, *Chemical Engineering Science*, 2003, 5299 – 5304.
41. Tai, Y., “Crystal growth kinetics of two step growth process in liquid fluidized bed crystallizer”, *Journal of Crystal Growth*, 1999, 109-118.

